



# VCU

Virginia Commonwealth University  
VCU Scholars Compass

---

Theses and Dissertations

Graduate School

---

2012

## CELL DEATH AND GROWTH ARREST PATHWAYS MEDIATING THE ACTIONS OF STILBENE 5C IN HCT-116 COLON CANCER CELLS

Moureq Alotaibi  
*Virginia Commonwealth University*

Follow this and additional works at: <https://scholarscompass.vcu.edu/etd>



Part of the [Medical Pharmacology Commons](#)

© The Author

---

Downloaded from

<https://scholarscompass.vcu.edu/etd/2851>

This Thesis is brought to you for free and open access by the Graduate School at VCU Scholars Compass. It has been accepted for inclusion in Theses and Dissertations by an authorized administrator of VCU Scholars Compass. For more information, please contact [libcompass@vcu.edu](mailto:libcompass@vcu.edu).

© Moureq Rashed Alotaibi 2012

All Rights Reserved

**CELL DEATH AND GROWTH ARREST PATHWAYS MEDIATING THE ACTIONS  
OF STILBENE 5C IN HCT-116 COLON CANCER CELLS**

A thesis submitted in fulfillment of the requirements for the degree of Master of Science in  
Pharmacology and Toxicology at Virginia Commonwealth University

by

**Moureq Alotaibi**

B.S. Pharmaceutical Sciences, King Saud University

Director: DR. DAVID GEWIRTZ,

Professor in Pharmacology and Toxicology

Virginia Commonwealth University

Richmond, Virginia

July 2012

## Table of contents

Page	
Acknowledgements.....	iv
List of figures.....	v
List of abbreviations.....	vii
Abstract.....	viii
<b>Chapter</b>	
1. Introduction.....	1
Cancer.....	1
Statistics.....	1
Colorectal cancer.....	2
Microtubule Inhibiting Agents .....	2
Stilbene compounds .....	3
Responses to Drug Treatment.....	5
2. Materials and Methods.....	12
3. Results.....	21
4. Figures.....	28-76
5. Discussion.....	77-86
References.....	87-91

## Acknowledgements

First, I would like to thank my parents for the endless support they have provided me with throughout my life, especially regarding my education. Although my father is no longer with us, while he was, he always encouraged me to push myself harder in order to reach my goals. I know that he would be proud to see how far I have come with my education. Also, my mother has always been a source of inspiration for me and I would like to thank her for constantly keeping me in her prayers and thoughts. I know my parents worked hard to help me get to the place that I am in at this point in my life, and for that I will always be grateful.

I would also like to thank my advisor, Dr. Gewirtz, for allowing me to join his lab since the summer of 2010. I appreciate the guidance he has given me throughout this process, without his help, it would not have been possible. He also provided me with the tools I needed in order to complete my work. I will not forget this and am thankful to be lucky enough to have had such a lab advisor.

Last, but not the least, I must thank King Saud University for awarding me with a scholarship and giving me the financial support that I needed in order to study abroad. In helping me to come to the US to study, the University enabled me to enrich my education in a way I never would have been able to do at home.

## List of Figures

<b>Figure 1.</b> Sensitivity of HCT116 cells to stilbene 5c .....	29
<b>Figure 2.</b> Determination of sensitivity to stilbene 5c based on clonogenic survival .....	31
<b>Figure 3.</b> Time course study of HCT116 cells after continuous exposure to 100 nM stilbene 5c.	33
<b>Figure 4.</b> Continuous exposure to stilbene 5c leads to loss of proliferation .....	35
<b>Figure 5.</b> Chronic treatment of 100 nM stilbene 5c promotes senescence in HCT116 colon carcinoma cells .....	37
<b>Figure 6.</b> Assessment of induced senescence by quantification of $\beta$ -galactosidase staining intensity in stilbene 5c-treated HCT116 cells .....	39
<b>Figure 7.</b> Evaluation of autophagy induction by acridine orange staining .....	41
<b>Figure 8.</b> Quantification of intensity of autophagy by flow cytometry .....	43
<b>Figure 9.</b> Stilbene 5c promotes the formation of red puncta with LC3-II in RFP-LC3 HCT116 colon cancer cells .....	46
<b>Figure 10.</b> Degradation of p62 protein after treatment of HCT116 cells with 100nM stilbene 5c .....	48
<b>Figure 11.</b> Assessment of apoptosis by detection of DNA fragmentation using the TUNEL assay .....	50
<b>Figure 12.</b> Stilbene 5c induces apoptosis in HCT116 colon cancer cells. ....	52
<b>Figure 13.</b> Mitotic catastrophe is promoted in HCT116 cells in response to 100 nM stilbene 5c.....	54
<b>Figure 14.</b> Stilbene 5c – treated HCT116 cells undergo mitotic catastrophe cell death. ....	56
<b>Figure 15.</b> Cell cycle analysis demonstrates growth and cell death in HCT116 colon cancer cells after exposure to 100 nM stilbene 5c .....	58
<b>Figure 16.</b> Similar response of p53-null HCT116 cells and p53-wt HCT116 cells to 100 nM stilbene 5c.....	60

<b>Figure 17.</b> Promotion of autophagy in p53-null HCT116 colon cancer cells after exposure to 100 nM stilbene 5c .....	62
<b>Figure 18.</b> Inhibition of colony formation in B16F10 melanoma cells by stilbene 5c .....	64
<b>Figure 19.</b> A dose-dependent decrease in colony formation in B16F10 in response to JG-03-14 .....	66
<b>Figure 20.</b> Stilbene 5c and JG-03-14 induce extensive autophagy in B16F10 melanoma cells ..	68
<b>Figure 21.</b> JG-03-14 and stilbene 5c promote senescence in B16F10 melanoma cells .....	70
<b>Figure 22.</b> Stilbene 5c did not suppress the metastasis of B16F10 melanoma cells in C57BL/6 mice.....	72
<b>Figure 23.</b> Evaluation of the effect of stilbene 5c on tumor growth and vascular perfusion ...	74
<b>Figure 24.</b> Images for B16F10 tumor nodules metastasized in mice lungs .....	76

## Abbreviations

D: day

St. 5c: Stilbene 5c

LC3: Light chain microtubule

RFP-LC3: Red fluorescent protein – LC3

TUNEL: Terminal deoxynucleotidyl transferase dUTP nick end labeling

DAPI: 4',6-diamidino-2-phenylindole

AO: acridine orange

MTT: 3-(4,5-dimethylthiazol-2-yl)-2,5-diphenyltetrazolium bromide)

DMSO: dimethyl sulfoxide



## CELL DEATH AND GROWTH ARREST PATHWAYS MEDIATING THE ACTIONS OF STILBENE 5c IN HCT-116 COLON CANCER CELLS

Alotaibi M.R.<sup>\*1</sup>, Xu Di,<sup>1</sup> Beckman M.J.<sup>2</sup>, Lee R. M.<sup>3</sup>, Gewirtz D.A.<sup>1</sup>,

### Abstract

The stilbene derivative, cis-3, 4', 5-trimethoxy-3'-aminostilbene (stilbene 5c), is a potentially potent antitumor agent that acts via binding to the colchicine-binding pocket in microtubules. Earlier studies have shown that stilbene 5c induces cell death in ovarian cancer cells and leukemic cells (Lee RM *et al*, 2008; Lee RM *et al*, 2008). The present study was designed to investigate the effectiveness of this microtubule poison against the HCT-116 human colon cancer cell line and its mechanisms of action. Time course studies demonstrated that stilbene 5c produces a biphasic decrease in cell viability. The capacity of the cells to proliferate was not restored upon removal of the drug after 6 days of exposure. Consistent with the results of the time course studies,  $\beta$ -galactosidase staining indicated that treatment with stilbene 5c also promotes senescence. In addition to senescence, stilbene 5c-treated HCT-116 cells displayed formation of autophagic vesicles by acridine orange staining, which was supported by fluorescence-activated cell sorting (FACS). Further evidence of autophagy was derived from treatment of HCT116 cells carrying an RFP-LC3 construct with stilbene 5c, in which LC3 puncta formation increased in a time-dependent manner. DAPI staining, TUNEL, and Annexin 5 staining indicated that apoptosis is also occurring in stilbene 5c-treated HCT-116 cells. Cell cycle analysis demonstrated growth arrest at both G1 and G2/M, and an increase in the subG1 population at days 3 and 5, which correspond to senescence and apoptosis respectively. Interestingly, DAPI and Hoechst staining revealed morphological changes in the cell nuclei (binucleated and micronucleated cells), which suggest that mitotic catastrophe may also serve as a mode of cell death after treatment with stilbene 5c. However, our studies indicated that stilbene 5c works in a p53-independent manner. Exposure of P53-null HCT116 cells to stilbene resulted in a similar sensitivity as in p53-wild type HCT116 cells. We found that autophagic vacuoles were formed in response to stilbene 5c in p53-null HCT116 cells as well. Consistent with previous studies in other experimental cancer models, this work indicates that stilbene 5c could potentially be effective against colon cancer through the promotion of multiple modes of cell death.

## Chapter 1: Introduction

### I. Cancer

Cancer is a set of diseases that result from abnormal growth of cells. Under normal conditions, differentiated cells divide and grow in a controlled manner to replace aged and damaged cells. When regulatory molecular mechanisms fail to manage the progression and growth of cells, newly developed abnormal cells will invade and destroy the surrounding tissues. Those abnormal cells gather to form a mass called a tumor. However, it is not necessarily that all formed tumors are cancers. There are also non life-threatening benign tumors that can develop by unusual progression of cells. Benign tumors are generally slower growing than malignant tumors. Also, benign tumors do not have the propensity to destroy or invade the adjacent organs and tissues, which all malignant tumors do. Cancer can develop in different organs and tissues, forming different kinds of malignant tumors. Another critical characteristic of malignant tumors is their ability to spread throughout the body in a process called metastasis. Metastasis occurs when cells migrate via the circulation and travel through the blood stream to another site. In the process of metastasis, cancerous cells can cause severe damage to essential organs such as the liver, the lungs, and the brain. (American Cancer Society)

### II. Statistics

Cancer is a serious health problem in the United States as well as throughout the world. Annually, one out of four deaths in the United States is cancer-related, signifying a high rate of mortality [1]. In the United States, 1, 638, 910 new cases of cancer were expected to be diagnosed and 577, 190 cases were anticipated to result in death[1]. The latest report has shown that there is a decrease in cancer incidence in different races and ethnicities during the last five years, especially in African American and Hispanics by 2.4% and 2.3%, respectively. Generally, cancers may be induced by natural radiation sources, environmental mutagens, viral infections, bacterial infections, fungal infections, and

failure of the immune system to prevent carcinogenesis. New reports indicated that colorectal cancer incidence is considered the third most common, as well as the third leading cause of death in both genders during the last few years.

### **III. Colorectal Cancer**

Colon carcinoma, sometimes called colorectal carcinoma, represents one of the most common and life-threatening cancers worldwide. Colorectal tumors are usually initiated by the development of noncancerous polyps in the tissues lining the colon. These developed polyps are subdivided into different kinds, and the polyps that most likely to develop into cancer are adenomatous polyps. According to the American Cancer Society ([www.cancer.gov](http://www.cancer.gov)), colorectal cancer is considered the third most diagnosed cancer as well as the third leading cause of cancer-related deaths in both genders in the US in 2011. Statistically, 141,210 cases are expected to be diagnosed with colorectal cancer and 49,380 deaths are caused by colorectal cancer. More than 20% of the cases presented in the clinic were late stage colorectal cancer which metastasizes to the liver. Typical therapeutic regimens for colon cancer include surgery, radiotherapy and chemotherapy. Although this type of cancer can be managed by surgery and/or chemotherapy, the late stages of colon cancer show high resistance to the current therapeutics. The first-line treatment of colon cancer includes a combination therapy of 5-fluorouracil, leucovorin, and oxaliplatin or irinotecan with bevacizumab [2]. However, treatment of patients with currently used chemotherapeutic agents is associated with severe side effects due to their cytotoxic effects on normal proliferating and resting cells. Hence, searching for new effective anticancer agents is necessary to overcome these major side effects.

### **IV. Microtubule inhibiting agents**

One of the major chemotherapeutic agents used to treat cancer is a class of drugs that interfere with microtubule function and inhibit normal cell cycle progression. Traditionally, microtubule poisons are categorized into two major groups: drugs that cause stabilization of microtubules such as taxanes and epothilones and drugs that destabilize microtubules such as vinca alkaloids and colchicines [3]. These microtubules inhibitors can also be classified into three classes according to their binding sites on microtubules [4]. Vinca alkaloids, which include vincristine, vinblastine, and vinorelbin, are effective in the treatment of haematological malignancies. Paclitaxel and docetaxel belong to a group named taxanes that are commonly used to treat ovarian cancer as well as breast cancer. Colchicine-site inhibitors are considered the third group of tubulin-binding inhibitors. Although many agents have been discovered and classified in the group of colchicines-site inhibitors (CSI), none of these compounds have been clinically approved. CA4P, a phosphorylated form of combretastatin, and ZD6126 have been tested in phase I human clinical trials and phase II for combretastatin only [5]. Clinical trials of these agents have shown their propensity to work as vascular disrupting agents (VDAs); however, CSIs have shown serious side effects such as neurotoxicity and cardiovascular toxicity [6-8]. Therefore, development of new colchicine-binding inhibitors with fewer side effects is important to effectively improve the therapeutic impact of outcomes of colchicine-site inhibitors.

## V. Stilbene compounds

Stilbene derivatives are a group of compounds that have established biological actions such as cell growth suppression and anti-vascular activities. A widely known agent of this group is trans-resveratrol (trans-3, 4', 5-trihydroxystilbene), a hydroxylated stilbene, that is found in grapes and possesses a beneficial effect in coronary artery disease [9]. Several studies have shown that resveratrol inhibits tumor cell proliferation in vitro and tumor vascularization in vivo leading to tumor growth

suppression [10]. Another example of biologically active stilbenes is combretastatin which is a natural cis-stilbene isolated from the South African tree *Combretum caffrum*. Previous studies have shown that combretastatin has potent anticancer properties via binding to tubulin, which in turn causes endothelial cell damage and neovascular disruption [11]. The structures of these compounds have been modified by Simoni et al., to synthesize therapeutically active analogs of resveratrol by the addition and removal of functional groups on the basic chemical structure [12]. This work resulted in the synthesis of many different compounds with variable potencies. Stilbene 5c and 6c were identified as the most two active compounds among them.

One of these newly developed compounds is cis-3, 4', 5-trimethoxy-3'-aminostilbene (stilbene 5c), a very potent inducer of tumor cell death via binding to the colchicine-binding pocket in microtubules [13]. This compound induces apoptosis in HL60 and U937 leukemic cells without producing cytotoxicity in normal haematopoietic progenitor cells at similar concentrations [14-15]. Also, stilbene 5c showed a very potent antitumor activity in SKOV3 ovarian cancer cells at low concentrations [14]. In vivo and in vitro studies have proven that stilbene 5c does not affect normal perfusion but disrupts the tumor vascularization, showing high selectivity against cancerous cells [16]. Moreover, stilbene 5c has a relatively wide therapeutic index; in vivo studies of stilbene 5c have indicated that the neurotoxicity starts at 100 mg/kg without observing cardiac or bone marrow toxicity, while a dose of 25 mg/kg has shown a therapeutic effect against ovarian cancer in treated mice [14]. In addition, the pharmacokinetic studies of stilbene 5c in tumor xenograft model indicated that the drug has an average half-life of 1.8 hours,  $C_{max}$  2,302 ng/mL and clearance 32.9 L/h [16]. In this study, the concentration of stilbene 5c was detected in brain, liver, spleen, heart, lung, kidney and plasma. Stilbene 5c levels were undetectable in lung, heart and spleen at 1 hour after the injection, but levels of stilbene 5c

in brain, liver and kidney were determined at 1 hour and significantly decreased 3 hours post injections. On the other hand, stilbene 5c was maintained accumulated in both plasma and tumor cells.

Stilbene 5c is thought to induce its anticancer effect in a cell cycle-dependent pathway since the drug is a microtubule poison. Stilbene 5c has been shown to block the progression of the cell cycle at the G2/M phase in several cell lines at low concentrations, while cell death was seen at higher doses [14]. A previous study indicated that stilbene 5c enhances the production of reactive oxygen species (ROS) through disturbing electron transport chain complex in mitochondria, which ultimately leads to cell death [14].

## **VI. Responses to drug treatment**

### **1) Apoptosis**

Apoptosis was first defined in 1972 by Kerr, Wyllie, and Currie to explain the characteristic aspects of programmed cell death [17]. It is a mode of cell death that takes place throughout the development as well as the growth and the aging of an organism. Apoptosis is considered to serve as a protective mechanism and healthy process that regularly occurs in living tissues to maintain the number of normal cells in that system in response to exposure to harmful signals or disease insults [18]. The morphological aspects of the dying cells have been differentiated between cells undergoing apoptosis and cells in necrosis. Unlike necrosis, apoptosis results in the reduction of cell size, cell nucleus, and rupture of nucleus and its chromatin, while oncotic necrosis is characterized by swelling and karyolysis [19]. Also, apoptosis is a controlled and energy-dependent cell death, which can occur in individual cells as

well as group of cells, whereas necrosis is a passive and uncontrolled process that can be due to e.g. a nonspecific injury to the cell membrane.

There are two types of apoptosis: physiologic and pathologic apoptosis. Either in physiological or pathological conditions, apoptosis can result from different types of stimuli affecting cellular signaling mechanisms and lead to a consequential cell death. It appears that apoptosis is a cell type specific process; that is some cell types are resistant to certain stimuli, while other cells may interpret the same stimuli as a trigger for death pathway induction. Physiologic apoptosis is an essential phenomenon that has been characterized in many human systems through developmental stages and adulthood in normal and disease states such as in the immune and nervous systems to kill pathogen-infected cells and overproduced cells [20-21].

Molecular mechanisms of programmed cell death are explored and well known. Apoptosis is an irreversible mode of cell death that involves caspase activation inside the cell and ends by engulfment of the apoptotic cell by macrophages. The process of apoptosis is composed of three phases that include initiation, effector, and degradation, where markers of apoptosis can be clearly identified. During this process, pro-apoptotic proteins stimulate upstream caspases to activate downstream effector caspases. Caspase cleavage leads to DNA cleavage by endogenous DNases that cut double strand DNA into fragments [22].

Apoptosis can be triggered by extrinsic and intrinsic pathways, where the former utilizes death ligand-death receptor binding, and the latter can be triggered by toxins or radiation. The extrinsic pathway involves the activation of a death receptor from the tumor necrosis (TNF) superfamily e.g. TRAIL. By activation, the adaptor molecule Fas-associated death domain (FADD) recruits caspase 8 and then initiates apoptosis via the cleavage of caspase 3 or 7. The

intrinsic pathway is generally triggered by the release of cytochrome c, smac/DIABLO, or apoptosis inducing factor (AIF) from the inner membrane of mitochondria. When a stress signal is initiated, those released mitochondrial proteins activate effector caspases and lead to subsequent DNA fragmentation [22].

It is noteworthy to mention that apoptosis plays a major role in various diseases. Dysregulations of programmed cell death is considered pathologic apoptosis that leads to many diseases such as cancer, autoimmune lymphoproliferative syndrome, AIDS, ischemia, and neurodegenerative diseases like Alzheimer's disease and Huntington's disease. Therefore, it is important to understand the molecular basis of apoptosis either to achieve a therapeutic effect of a drug or to better know how biological systems respond to abnormal cell division.

## 2) Autophagy

Autophagy is a biological process that is induced upon nutrient deprivation and/or cellular stress. During autophagy, intracellular and extracellular nutrients are sequestered into autophagosomes and transported to the lysosomes to be degraded, recycled, and then reused by the cell. Autophagy plays key roles in regulation of cellular homeostasis by breaking down old or misfolded proteins, maintaining the viability of starving cells by producing amino acids, and protecting cells against pathogenic infections by the engulfment of a pathogen [23-25]. Cells that undergo autophagy are characterized by enlargement and swelling of nuclei with formation of acidic vacuoles. Although the role of autophagy is still debatable, several reports indicated that autophagy is a protective process induced to maintain cellular viability in response to harmful insults [26-28].



Promotion of autophagy is highly regulated by different genes and advances through several steps: induction, autophagosome nucleation, and completion, by which formed autophagosomes fuse with lysosomes for protein breakdown [29]. During the first phase, the Atg1 complex, which includes Atg1, Atg13, and Atg17 as well as other factors, is activated to initiate autophagy [30]. Then, class-III phosphatidylinositol-3-kinase (PI3K) and Beclin-1/Atg6 activation is required to collect parts of cytoplasm and other organelles and build up a double-membraned autophagosome. After that, LC3 protein is cleaved by Atg4 protease and lipidated by phosphatidylethanolamine (PE) via Atg7 and Atg3 proteins to form LC3-PE. Following LC3 cleavage, the Atg12/Atg5/Atg16 complex regulates the binding of LC3-PE to the autophagosomal membrane [31-33]. Finally, formed autophagosomes unite with acidic lysosomes, which results in the decomposition of autophagosomes-sequestered proteins [25-26].

An important regulator protein of autophagy is the mammalian protein kinase mTOR, which is the target of rapamycin. mTOR protein is a serine/threonine kinase that is activated under healthy growth conditions and induces gene translation and synthesis of necessary proteins. During starvation and nutrients deprivation, the mTOR pathway becomes inactivated and autophagy is promoted [34]. Also, PI3K pathway functions upstream of mTOR to contribute to autophagy induction [35-36]. This pathway is shown to be activated due to nutrient deprivation but not in response to conventional chemotherapy. Therefore, it could be valuable studying the activation of these pathways by the effects of microtubule inhibitors.

### 3) Senescence

Senescence is considered to be an irreversible growth arrest of cells. During senescence, the cells' shape and morphology become flattened and enlarged with decreased pH and enhanced

$\beta$ -galactosidase activity [37]. Generally, senescent cells show resistance against mitogenic and apoptotic signals [38]. Senescence occurs as a result of oncogenic stress, DNA damage, or cytotoxic drugs [39]. However, irregular senescence is associated with the development of certain diseases such as atherosclerosis, osteoarthritis, muscular degeneration, ulcer formation, Alzheimer's dementia, diabetes, and immune exhaustion [40]. On the other side, defective signaling pathways of senescence may lead to unlimited growth of cells, which may ultimately form a tumor. The ability of these cells to become immortal results from the fact that cancer cells are capable of escaping from the regulated lifetime of somatic normal cells. Thus, cellular senescence is thought to be a tumor suppressing process as it stops infinite cellular divisions [41].

To determine a finite number of cell divisions, the term "*Hayflick limit*" is used as a reference for how many times a normal cell will divide. Every chromosome has a structure at the end of its DNA called the "Telomere" which contain repeat of the sequence TTAGGG [42-43]. The telomere is not replicable, and therefore becomes reduced after each cell division. The decrease in telomere length eventually limits the ability of cells to divide. Therefore, the reduction in telomere length is considered as an important factor in the regulation of replicative senescence [44].

Senescence can be induced via many pathways [40], but the two major pathways that are involved in senescence are: p14ARF/p53/p21 pathway and the INK4/CDK/pRb pathway [45]. In the first pathway, the protein p14ARF negatively regulates MDM2, which originally ubiquitinates p53, and thus causes activation of p53 [46]. Consequently, the p53 protein acts upstream of a CDK inhibitor p21, leading to growth arrest and senescence [47]. Also, p53 has other downstream targets to promote cellular senescence such as 14-3-3 and GADD45 that

inhibit G2/M transition and downregulation of *myc* [48]. In the pRb-dependent pathway, senescence-inducing signals activate p16INK4a that inhibits the function of CDKs. The pRb protein is known to be inactivated by CDKs; consequently, p16INK4 activation promotes Rb dephosphorylation and Rb activation to bind to members of the E2F family of transcription factors, which results in cellular senescence [49-50]. Furthermore, there is a cross-talk between these two pathways. The protein p21, which is upregulated by p53, promotes senescence either directly by the first pathway or through the inhibition of CDK in the second pathway [51].

Senescence can be telomere-dependent or –independent. Telomeres are gradually lost in each S phase of cell cycle, resulting in loss of DNA at the very end of chromosomes. Also, some cells lack the ability to reactivate telomerase, the enzyme responsible for the addition of DNA sequence repeats at the end of chromosomes [52-53]. Existence of erosions at telomeric sites leads to the generation of a persistent DNA damage response and growth arrest [54-56]. In addition, nontelomeric DNA breaks can induce senescence and growth arrest via persistent DNA damage response [57].

Senescence can also occur independently of the DNA damage response. Several reports have indicated that p21WAF1 and p16INK4a can induce cells to undergo senescence with no DNA damage response [55, 58]. A kind of stress called “Culture shock” induces senescence with no erosions of the telomeres [59]. This group of stresses includes hyperphysiological oxidation and the presence of serum instead of plasma. Furthermore, loss of Pten phosphatase also causes growth arrest of cells without induction of the DDR signaling pathway [60].

Although stilbene 5c is not a DNA damaging agent like some anticancer drugs and ionizing radiation, it could induce senescence through the activation of some tumor suppressor

genes. Many reports indicated that some microtubule poisons lead to cell division failure accompanied with activation of check points [61-62]. Therefore, it is worthy to study whether stilbene 5c promotes senescence in HCT116 colon carcinoma cells.

#### 4) Mitotic catastrophe

Mitotic catastrophe is a term used to describe a mode of cell death resulting from dysregulated mitosis, usually resulting in the formation of cells with multiple nuclei. During mitotic catastrophe, clusters of aneuploidy and missegregated chromosomes are formed and enclosed within the nuclear envelope. The formation of the nuclear envelope results in the enlargement of treated cells with the presence of multiple micronuclei, as a distinct feature of mitotic catastrophe. Also, mitotic catastrophe induction can be determined through the expression of mitosis-related genes. This faulty mitosis occurs as a result of disconnection between the phase of DNA replication and mitosis during cell cycle progression. Thus, it is still controversial whether mitotic catastrophe is a mode of cell death or a phenomenon that leads to cell death via apoptosis or necrosis [63]. It is worth mentioning that cancer cells need to escape apoptosis to develop malignancy. Despite the differences between mitotic catastrophe and apoptosis, several reports have shown that drug-induced mitotic catastrophe is associated with the release of pro-apoptotic proteins and activated caspases, indicating similarity in signaling pathways, or at least a cross-talk between apoptosis and mitotic catastrophe [64-66]. Many reports have shown that mitosis-regulating proteins have been changed in response to antitumor drugs, thus leading to an aberrant mitosis and nuclear division [67-69]. The clinical significance of mitotic catastrophe as a mode of cell death is derived from evidence of mitotic catastrophe formation beside other modes of cell death in cancer patients treated with antitumor drugs [67, 70-71]. Several anti-microtubule agents such as vinca alkaloids and taxanes have been shown to

promote mitotic catastrophe probably by mitotic spindles disruption [71-72]. Given the fact that stilbene 5c is a microtubule poison, it is important to address whether this drug induces mitotic catastrophe in HCT116 cells.

## Chapter 2: Materials and methods

### 2.1 Cell culture

HCT-116 colon cancer cells were purchased from ATCC and maintained in 10% DMSO (Sigma Chemical, St. Louis, MO) with Fetal Bovine Serum (FBS) (GIBCO Life Technologies, Gaithersburg, MD) and stored frozen in liquid nitrogen until ready for use. Cells were defrosted and cultured in a T75 flask (Cellstar) in RPMI 1640 medium with 5% fetal bovine serum, 5% bovine calf serum, 2 mM L-glutamine, and penicillin/streptomycin 0.5 mL/100 mL medium (10,000 units/mL penicillin and 10 mg/mL streptomycin (GIBCO Life Technologies, Gaithersburg, MD) and incubated at 37°C, 5% CO<sub>2</sub>, in a moisturized environment. When cells reach 80% confluency, cells are washed with 1X PBS (GIBCO) and harvested by 0.25% trypsin-EDTA (GIBCO) (incubation for 5 minutes). Trypsin is deactivated by addition of 5 mL of serum-containing RPMI 1640, cells are collected and centrifuged at 1,500 rpm for 5 minutes. Media and trypsin are removed and 5 mL of new sterile medium is added to the pellet; cells are resuspended and 500 µL of suspension is placed into 96 mm<sup>3</sup> plate filled with 10 mL of RPMI 1640 medium. In every experiment, cells are cultured under identical conditions and incubated overnight to allow for adherence before treatment with continuous drug exposure. Stilbene 5c preparations were kindly provided by Dr. Ray Lee's laboratory at Virginia Commonwealth University. Drug was diluted in autoclaved DMSO (Sigma Chemical, St. Louis, MO) aliquots at concentrations of 30 mM and 300 µM. Used drug was not thawed more than twice due to the stability of the drug.

## *2.2 Clonogenic Survival assay*

The ability of cells to form colonies was evaluated by plating 200 cells in 6-well plates for control, 1% DMSO, 10 nM of stilbene 5c, and 30 nM of stilbene 5c, and 2000 cells for 100 nM of stilbene 5c, 300 nM of stilbene, and 600 nM of stilbene 5c. Cells were permitted to adhere for overnight. The next day, cells were treated with the indicated concentrations for 2 days, drug was removed and fresh media was added every other day. At day 9, cells were washed one time with 1X PBS before fixation with 100% of methanol for 10 minutes. Methanol was aspirated and colonies were stained with crystal violet dye (1%) in deionized water for 10 minutes. Colonies were counted visually in each well.

## *2.3 MTT dye assay for cell viability*

In 96-well plates, 200  $\mu$ L of medium containing 6000 cells was added to each well and left to attach overnight prior to drug treatment. After 72 hours of drug exposure, media was aspirated and MTT solution (2 mg/mL PBS made up in the dark) was added to each well and incubated at 37°C for 3 hours. The MTT dye becomes reduced to insoluble formazan inside living cells. 100  $\mu$ L of DMSO was added for 5 minutes to each well to dissolve the blue dye. Absorbance was read at 490 nm (KC Junior software, EL800 Universal Microplate Reader).

## *2.4 Time course of drug toxicity and its impact on cell viability*

Cells were cultured in 6-well plates in equal number and left overnight for attachment. The next day, cells were treated with drug and the number of viable cells was counted on daily basis for 5 days. At every time point, drug was removed and cells were washed one time with 1X

PBS. Then, 350  $\mu\text{L}$  of 0.25% trypsin was added to every well for harvesting and incubated for 5 minutes, then deactivated by 650  $\mu\text{L}$  of fresh media, to make up 1 mL of cell suspension. Cells were collected in 1 mL conical tubes (Eppendorf) and 10  $\mu\text{L}$  of cell suspension was added to 10  $\mu\text{L}$  of trypan blue and injected in chamber slides (invitrogen) and counted using Countess Machine (invitrogen). A compromised cell membrane will allow trypan blue to penetrate inside the cell, indicative of loss of viability.

### *2.5 Assessment of apoptosis by DAPI staining*

At indicated time points, both adherent and non-adherent cells were collected and centrifuged at 1,500 rpm for 5 minutes. Medium was removed and cells were resuspended in 1 mL of fresh medium. Cells were then diluted to 40,000 cells in 200  $\mu\text{L}$  of 1X PBS and the same volume was loaded per slide. Prepared slides were spun at 3,000 rpm for 5 minutes (Shandon Cytospin 4, Thermal Electron Corp). Slides were kept in refrigerator until ready for experimental use. At the day of staining, cells were fixed at room temperature with 4% formaldehyde in 1X PBS for 10 minutes. Slides were then rinsed in 1X PBS for 10 minutes. Acetic acid was diluted in ethanol (1:2 dilution) and used to fix cells at 20°C for 5 minutes and then washed with 1X PBS for 5 minutes. 10  $\mu\text{L}$  of Vectashield:Dapi (1:1000 dilution) was prepared and added to every slide. Nail polish was used to seal slides with cover slips. Images were taken using an Olympus 1X 70 microscope and an Olympus SC 35 type camera. Three different experiments were visualized and assessed.

### *2.6 TUNEL assay for apoptosis*

Another method of assessments of apoptosis is by detecting DNA fragmentation via Terminal deoxynucleotidyl transferase dUTP nick end labeling (TUNEL). For this assay, cells



were harvested and collected at various time points and centrifuged at 1,500 rpm for 5 minutes. Medium was removed and cells were resuspended in fresh media. A dilution of 40,000 cells in 200  $\mu$ L per slide was prepared and cells were spun at 3,000 rpm for 5 minutes (Shandon Cytospin 4, Thermal Electron Corp). Slides were kept refrigerated at 4°C until ready for use. On day of staining, cells were washed with PBS and then fixed with 4% formaldehyde in PBS for 10 minutes at room temperature. Cells were then washed twice with PBS for 5 minutes and fixed with 1:2 of acetic acid and ethanol for 5 minutes at 20°C, and washed again with PBS. ImmunoPen was used to surround cells and hold solutions. After that, cells were blocked with BSA diluted in PBS in a ratio of 1 mg/ml for 30 minutes. Slides were rinsed twice in PBS and enzyme mixture composed of 5X buffer, terminal transferase, 25mM CoCl<sub>2</sub>, fluorescein-12dUTP and deionized water, was added for staining for an hour in incubator. After two washes with PBS, slides were topped with cover slips and images were taken under the fluorescence microscope. The same slides could be used for DAPI staining by mounting with Vectashield: DAPI (1:1000) before cover slips.

### *2.7 Annexin 5-PI staining for apoptosis*

In cells undergoing early apoptosis, phosphatidyl serine (PS), which is originally located in the inner cell membrane, transfers to the outer cell membrane. Translocated phosphatidyl serine (PS) can be bound with Annexin V attached to a fluorescent chromophore (FITC) to identify early apoptosis. Propidium iodide (PI) penetrates non-intact cellular membranes and stains cells, serving as a marker of late apoptosis or necrosis. In this experiment, cells were plated overnight to permit cells to adhere. On the following day, cells were treated with the drug. At several time points, adherent and non-adherent cells were harvested by 0.25% trypsin and centrifuged at 2,000 rpm for 5 minutes. Cells were then resuspended in 1 mL of 1X PBS,

transferred to 2 mL tubes, and centrifuged at 2,000 rpm for 5 minutes. PBS was removed and 100  $\mu$ L of 1X binding buffer (BD Biosciences) was added to pellets per tube. 5  $\mu$ L of Annexin-FITC (BD Biosciences) and 5  $\mu$ L of PI at 10  $\mu$ g/mL (BD Biosciences) were then added per tube. In the dark, cells were softly vortexed and incubated for 15 minutes at room temperature. Before analysis by flow cytometry, 400  $\mu$ L of 1X binding buffer was added per tube and samples were analyzed by flow cytometry technique as soon as possible to measure the fluorescence at 530 nM.

### *2.8 Hoechst Staining for mitotic catastrophe*

Both adherent and non-adherent cells were both harvested at indicated time points and centrifuged at 1,500 rpm for 5 minutes at 5°C. Supernatant was removed and the cell pellet was resuspended in 5 mL of PBS diluted to 40,000 cells in 200  $\mu$ L, and refrigerated. On the day of staining, cells were fixed with 0.075 M KCL for 8 minutes at room temperature, and then washed with 1X PBS. A 1:3 dilution of methanol and glacial acetic acid was prepared and slides were rinsed in solution for 20 minutes and then washed with deionized water and allowed to dry overnight. Cells were stained with Hoechst dye of 2  $\mu$ M in nanopure water for 10 minutes and slides were topped by cover slips and images were taken by the same tools as for DAPI and TUNEL. Mitotic catastrophe was evaluated according to the formation of bi- and micronucleated cells.

### *2.9 Evaluation of autophagy by acridine orange staining*

200,000 cells were seeded in 6-well plates and permitted to adhere overnight and drug-treated the next day. At various time points, drug was removed and cells washed once with 1X PBS. Acridine orange dye was diluted in PBS in a ratio of 1:10000 (prepared in the dark) and

added to cells for staining, and incubated for 15 minutes. Dye then was aspirated and plates were washed with 1X PBS and fresh medium was added. Photographs were taken with an Olympus 1X 70 microscope and an Olympus SC 35 camera.

### *2.10 Transfection of HCT116 cells with RFP-LC3*

The Tolkovosky laboratory has generated the RFP-LC3 construct [73]. Frozen cells were thawed, centrifuged, placed in a fresh medium, and passaged many times before transfection.  $1 \times 10^6$  cells were collected in a pellet and resuspended in 100  $\mu$ L of the Nucleofector V mix (Nucleofector kit V, Amaxa). A microgram of the RFP-LC3 vector was added to the suspension. The whole entire suspension was transferred to a cuvette, which then was placed in the nucleofector device to run program D-32 and transfect the cells. Transfected cells were then mixed with 500  $\mu$ L of warm medium and transferred to a Petri dish. Gentamycin 8ng/mL was used to maintain a stable transfection.

### *2.11 Measurement of acridine orange staining by flow cytometry for autophagy*

Flow analysis was utilized to count the cell population positively stained with acridine orange. Treated cells were harvested, collected, and centrifuged at speed of 1500 rpm. Supernatant was removed and pellets were resuspended in 1 mL of fresh medium. Cell suspension was filtered through standard flow cytometry 40 micron filter (BD falcon). A 10:1000 dilution of acridine orange in 1X PBS was prepared (in the dark) and protected from light until ready for use. At flow cytometry, 10  $\mu$ L of acridine orange solution was added to per sample to make the dilution of 1:10000. When analyzed by flow cytometry, the acridine orange dye is excited at wavelength 525 nM for green fluorescence and 620 nM for red fluorescence.

### *2.12 Senescence by $\beta$ -Galactosidase staining*

Detection of senescence was by  $\beta$ -Galactosidase staining after exposure to the drug treatment. Cells were washed once with 1X PBS and fixed with 2% formaldehyde/ 0.2% glutaraldehyde for 5 minutes. Fixing solution was aspirated and PBS was used again to wash and a staining solution composed of 1 mg/mL 5-bromo-4-chloro-3-inolyl- $\beta$ -galactosidase in dimethylformamide (20 mg/mL stock), 5 mM potassium ferricyanide, 150 mM NaCl, 40 mM citric acid/sodium phosphate, 2 mM MgCl<sub>2</sub>, at pH 6.0 was added and the cells were incubated overnight at 37°C. The following day, cells were washed twice with PBS and pictures were taken.

### *2.13 Quantification of $\beta$ -Galactosidase staining using flow cytometry for senescence*

On the day of staining, old media was washed out and 100 nM of bafilomycin A1 in fresh media was added to the treated cells to induce lysosomal alkalization and left incubated at 37°C and 5% CO<sub>2</sub> for 1 hour. After incubation, C<sub>12</sub>FDG working solution was added to each well in amount to make the final concentration 33  $\mu$ M and was continued incubation for another 1 hour. Media was then aspirated and cells were washed twice with PBS. Cells were harvested and collected for centrifugation at speed 1500 rpm and resuspended in PBS. C<sub>12</sub>FDG is a substance that hydrolyzed by upregulated  $\beta$ -galactosidase enzyme and becomes fluorescent at wavelength of 500–510 nM.

### *2.14 Cell cycle analysis*

Cells were seeded overnight to adhere. The next day, supplemented medium was removed and serum depleted medium was added and left for 24 hours to synchronize all cells at the same phase. On day 0, cells were treated with stilbene 5c. At the indicated time points, viable

and non-viable cells were harvested and collected. Cells were centrifuged at 1500 rpm and supernatant was aspirated. Pellets were resuspended in PBS for wash and centrifuged at 1500 rpm again. After removing supernatant, 0.2 mL of PBS was added and pellets were resuspended very well in order to obtain a single cell suspension. 1.8 mL of cold 70% ethanol was added gradually per tube into the cell suspension and vortexed very well. Cell suspensions were stored at 4°C until ready for use. On day of staining, cells were centrifuged from ethanol and PBS was added for wash. PBS was removed and staining solution was added to the pellets 2 hours prior to flow cytometry. Staining solution contains 0.1% (v/v) Triton-X-100 in 10 mL PBS, 2 mg of DNase-free RNase A, and 0.2 mL of the propidium iodide stock (1 mg/ml).

## *2.15 Assessment of antitumor effect of stilbene 5c in vivo*

B16F10 melanoma cell line is murine malignant tumor cells that can be injected in the C57BL/6 mouse to form a syngeneic model. This cell line was chosen for its ability to metastasize into the lungs. In this study, mice were injected with  $1 \times 10^5$  tumor cells/mouse on day 29. In the following day, mice were intraperitoneally injected with the drug once a day, five days a week, for two weeks. The drug was diluted in a vehicle containing Tween, Ethanol, and saline in a ratio of 2:1:7 respectively. Sentinel mice were used to monitor the formation of tumor nodules onto the lungs. At certain time point, mice were sacrificed and the lungs were removed and saved in Bouin's solution, a common fixative solution used to preserve tissues. The tumor burden in mice was assessed based on two parameters. The first parameter is the visual counting of how many black nodules have been formed in each lung. The second parameter was used is the calculation of the surface area of each nodule. Measurement of the latter parameter was performed by embedding lung tissues into paraffin, sectioned at 4 microns thickness and stained with Hematoxylin and Eosin. Images of stained nodules were taken under the microscope and

the surface area of each tumor nodule was calculated using Nanozoomer computer software (Olympus).

### *2. 16 Western blotting*

In order to determine whether some proteins were induced, degraded, or downregulated, we conducted a specific assay to analyze protein levels. After the indicated time points, we collect viable and non-viable cells in a pellet. These collected cells were mixed with 100 to 200  $\mu$ L of 1X Tris lysis buffer (1 M Tris (pH 6.8), 10% SDS, and dH<sub>2</sub>O) containing protease inhibitors and boiled for 5 minutes. Protein concentration was measured using the Bradford protein assay (BioRad) and 40  $\mu$ g of total cell lysate was separated in a 12% gel using SDS-PAGE. Proteins were transferred onto nitrocellulose membrane for 1.5 hours and washed 3 times with PBS containing 0.01% Tween for 5 minutes in each time. Membrane was blocked for one hour with TBS-Tween 20 buffer containing 5% nonfat dry milk. The proteins were then blocked with the primary antibody and left overnight in 4°C. In the following day, the primary antibody was washed out and the immunofluorescent secondary antibody was added for an hour at room temperature. Membrane was washed three times and bands were detected using enhanced chemiluminescence detection reagents from Pierce (Rockford, IL).

### *2. 17 Statistical analysis*

Statistics were performed using ANOVA followed by post-hoc analysis. The significance of group values was determined based on a p-value of  $p < 0.05$ .

## Chapter 3: Results

### *3.1 Stilbene 5c produces growth arrest and cell death in HCT116 colorectal cancer cells.*

Previous reports have shown that stilbene 5c was effective in promoting cell death and growth arrest at nanomolar concentrations, 30 nM and 100 nM, showing high potency against both leukemic and ovarian cancer cells [8-9]. Figure 1 show that continuous exposure of HCT116 cells to 0, 30, 100, 300, and 600 nM of stilbene 5c for 72 hours resulted in reduced numbers of viable cells in a dose-dependent manner, with a significant cell viability decrease at 100 nM, 300 nM, and 600 nM by approximately 75%, 80%, and 84%, respectively. Consistent with our observation in the MTT assay, treatment of HCT116 colon carcinoma cells with stilbene 5c for 48 hours with the same indicated concentrations resulted in a 90% decline in colony formation starting at 100 nM (Figure 2). This concentration is relevant to the plasma concentration that has been shown previously in the pharmacokinetic studies of stilbene 5c in mice [16]. Based on these findings, we have chosen to continue our work with 100 nM as our effective concentration to further investigate the mechanisms of drug's cytotoxicity. In order to understand whether stilbene 5c induces cell killing or growth arrest, we assessed the effects of stilbene 5c on cell viability over a period of five days in a time course study. Figure 3 demonstrates a decrease in number of viable cells in a time course treatment when exposed to 100 nM stilbene 5c. Twenty-four hours post treatment, extensive cell death was observed in the treated groups. Thereafter, the treated tumor cell populations showed an apparent prolonged growth arrest. To assess whether treated HCT116 cells were able to recover their capacity to proliferate, drug was washed out on day 5 and fresh medium was added and replaced every other day for an additional 10 days. These experiments demonstrate that the residual surviving tumor

cell population had lost its capacity to recover, pointing toward an irreversible growth arrested state.

### *3.2 Induction of irreversible senescence and loss of proliferation*

In previous studies, UCI-101 and SKOV3 ovarian cancer cells and HL60 and U937 leukemic cells displayed a growth suppression and cell cycle arrest at G2/M upon treatment with stilbene 5c [8,9]. In our time course study, cells treated with 100 nM of stilbene 5c have shown cell death followed by growth arrest during days 2, 3, and 4. In addition, residual cells did not show proliferative recovery after drug removal by 10 days (Figure 4). Therefore, we decided to determine whether senescence was promoted in response to the treatment with stilbene 5c.  $\beta$ -galactosidase staining was performed 72 hours post treatment and visualized by microscopy. Treated groups showed morphological markers of senescence such as granulations, flattening, and spreading of cells. Also, the treated cells demonstrated positive staining with bluish green  $\beta$ -galactosidase color (Figure 5). The intensity of  $\beta$ -galactosidase staining was further quantified by flow cytometry technique on days 2 and 4 (Figure 6A). A significant fraction of the treated cell populations was apparently shifted to the area of positive staining with a rightward move of the histogram peak on day 4, but not on day 2. In addition to the quantification of  $\beta$ -galactosidase staining, flow cytometry technique also was used to measure the size of cells. Treated HCT116 colon carcinoma cells on days 2 and 4 were remarkably enlarged compared to control (Figure 6B), showing consistency with our microscopic observations. Taken together, senescence was initiated in HCT116 cells as early as 48 hours after initiating the treatment with stilbene 5c.

### *3.3 Promotion of autophagy by Stilbene 5c in HCT116 cells*



Autophagy is a regulated process in which misfolded proteins and damaged cellular components are broken down by lysosomal enzymes in double-membrane enclosures. Some literature reviews and studies indicate that extensive autophagy is defined as type II programmed cell death. However, a recent study showed that the process of autophagy is an important mechanism that leads to senescence [74]. In addition, previous studies from our laboratory demonstrated that autophagy and senescence were induced in HCT116 cells in response to another colchicine site-binding inhibitor, JG-03-14. Since stilbene 5c induced senescence in HCT-116 colon carcinoma cells, we then sought to establish whether senescence might be preceded by autophagy. A number of different approaches and tools including acridine orange staining, RFP-LC3 redistribution, and p62 degradation were utilized to address this question.

During autophagy, acidified autophagosomes fuse with lysosomes to form acidic vacuoles, which are stainable by acridine orange dye. Figure 7 shows that control HCT-116 cells have a single orange circle per cell located approximately in the same site in the cytoplasm, indicating a relatively high basal level of autophagy that may be induced in HCT-116 cells due to activated *ras* protein [75]. Cells treated with 100 nM of stilbene 5c displayed different large number of stained vacuoles per cell that increased in a time-dependent manner. In addition, cells exposed to 100 nM of stilbene 5c became enlarged in comparison with control cells, demonstrating a morphological sign of autophagy. An additional flow cytometry technique used to evaluate autophagy in cells based on the intensity of acridine orange staining was used in our studies. In this experiment, we found that treated cells showed a significant increase in the percentage of the cell population falling into the area red-fluorescing cells ( $5.3 \pm 3.03$  with control,  $25.07 \pm 6.26$  with treatment;  $p < 0.05$ ), indicating cells undergo autophagy when treated with stilbene 5c (Figure 8).

We also monitored the localization of the LC3-II protein in HCT116 colon carcinoma cells. LC3-I is a cytoplasmic protein that converts to LC3-II when lipidated and binds to autophagosomal membranes during autophagy. On days 1, 2, and 3, RFP-LC3 - transfected HCT-116 cells were visualized by fluorescent microscopy. As shown in figure 9, promotion of autophagy was confirmed by RFP-LC3 redistribution. Whereas control cells show one small diffuse fluorescent punctate per cell, red puncta were clearly increased and distributed in the treated cells.

Autophagic flux was also measured via p62 degradation, a protein sequestered in autophagosome and degraded by lysosomal hydrolases [76]. HCT116 colon cancer cells treated with 100 nM stilbene 5c were tested for p62 decomposition by immunoblotting. Level of p62 clearly declined 48 hours post treatment (Figure 10).

### *3.4 Evaluation of apoptotic cell death induced by stilbene 5c*

One of the desirable outcomes of therapeutic treatment of cancer is the promotion of apoptosis. We evaluated apoptosis in HCT116 cells in response to 100 nM of stilbene 5c via different assays including DAPI staining, TUNEL assay, and Annexin V-PI staining. Even though we observed cell death during the first day in our time course study, we failed to find any evidence of apoptosis 24 hours after the treatment with stilbene 5c in our annexin V-PI staining experiment (Figure 12). Dramatically, a significant part of the treated cell population shifted toward early and late apoptosis on days 3 and 5 ( $4.2 \pm 3.63$  with control,  $3.533 \pm 0.321$  with Day 1,  $19.6 \pm 4.6$  with Day 3,  $19.6 \pm 1.77$ ;  $p < 0.05$  control versus Day 3 and Day 5). To confirm the induction of apoptotic cell death in cells treated with stilbene 5c, we stained cells with DAPI and

TUNEL to characterize apoptosis markers under the fluorescent microscope. Although DAPI staining barely shows nuclear shrinkage or distortion in treated groups, TUNEL images for the same samples presented fluorescence of fragmented DNA, indicating that HCT116 cells undergo apoptosis upon drug treatment (Figure 11).

### *3.5 Assessment of mitotic catastrophe by stilbene 5c*

In addition to apoptosis, there is another form of aberrant mitosis – caused cell death known as mitotic catastrophe. Several reports have shown that mitotic catastrophe might characterize a mitotic form of apoptosis [65, 77]. In our assessment of apoptosis markers by DAPI staining, we found that some cells have abnormal nuclear morphology that was obviously enlarged with multipolar structure. We then plated HCT116 cells in 6-well plates and treated them with 100 nM stilbene 5c. Cells were then stained directly with DAPI while they were in the plates. Images of DAPI confirm mitotic arrest in treated cells as shown by the appearance of more than a single nucleus in one cell (Figure 13). Therefore, we performed another experiment called Hoechst staining to ensure that this finding is not only restricted to DAPI staining as well as to prove that mitotic catastrophe is induced in stilbene 5c-treated cells. Figure 14 demonstrates that treated cells have bi- and micronuclei with the presence of DNA fragments as an indication of mitotic catastrophe induction.

### *3.6 Stilbene 5c induces p53-independent cell death*

Due to the appearance of multiple modes of cell death in HCT116 cells in response to stilbene 5c, we then sought to investigate the role of the wild-type p53 gene in HCT116 cells and the involvement of this protein in the antitumor action of stilbene 5c. The tumor suppressor gene p53 plays major roles in cell mechanisms that respond to a genotoxic stress such as the induction of cell cycle arrest at G1/S phase and the initiation of apoptosis signaling pathways. It has been widely known that cells lack wild-type p53 have the capability to evade apoptosis and become more likely to be resistant to anticancer therapy. Thus, one of the most desirable effects of an antitumor agent is to be working regardless p53 status since more than 50% of tumor cell lines are p53 mutant. In order to understand the function of p53 in our system, we treated HCT116 (p53 -/-) cells with 100 nM stilbene 5c and evaluated the cell viability in a time course study. (p53 -/- HCT-116) cells showed equal sensitivity to stilbene 5c as in the p53 wild-type HCT-116 cells, indicating that stilbene 5c does not require a wild-type p53 gene to produce its anticancer effect (Figure 16).

### *3.7 Induction of autophagy in HCT116 (p53 -/-) and HCT116 (p53 +/+) cells*

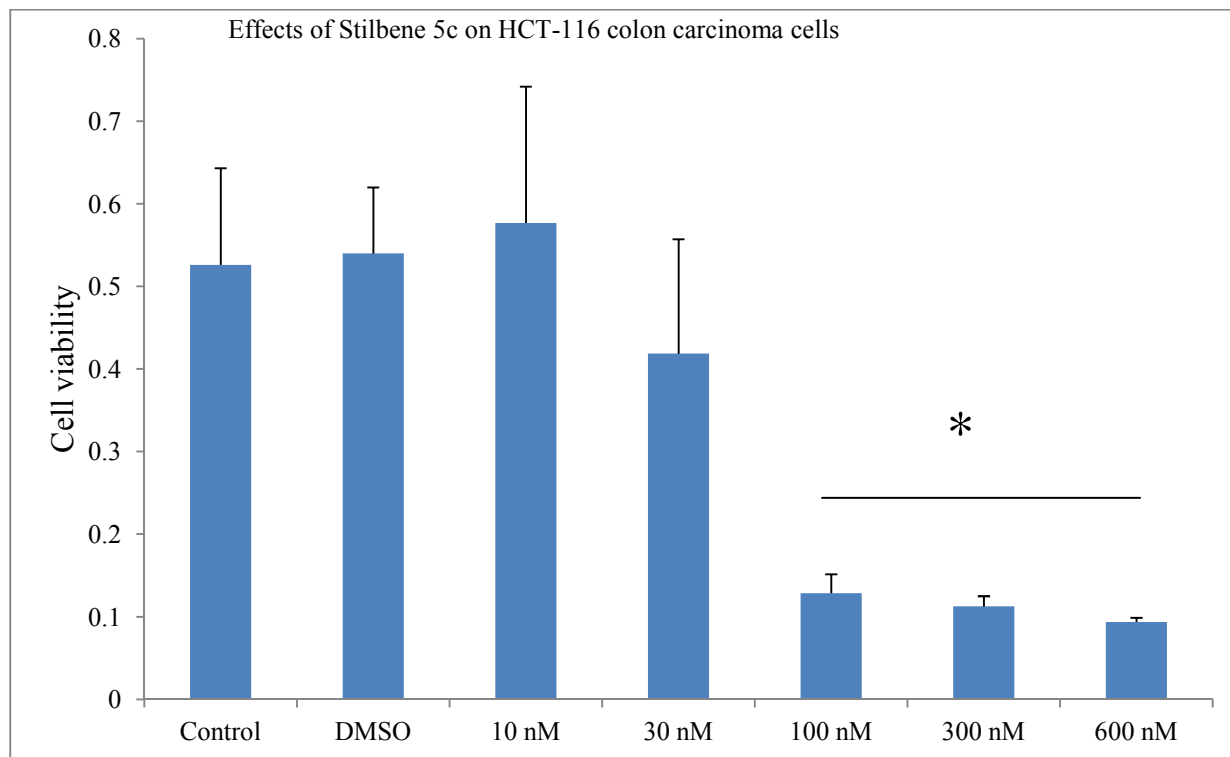
As we observed that stilbene 5c is also effective in p53-null HCT116 cells, we wanted to identify the early mode of cell death in those cells. Our previous results indicated that apoptosis was not evident in HCT116 (p53 +/+) cells until day 3. Therefore, it was important to perform similar studies in the p53 null cells using acridine orange staining to determine whether autophagy is induced in order to better understand the role of autophagy in our system. We found that extensive autophagy is promoted at the same extent in both p53-null and wild type cells

during the first three days (Figure 17). This finding may point toward the probability of autophagic cell death in HCT116 cells as a result of stilbene 5c treatment.

### *3. 8 Low dose of stilbene 5c does not disrupt tumor vascularization and fails to inhibit metastasis of B16F10 melanoma cells in C57BL/6 mice*

The effectiveness of stilbene 5c was also examined in B16F10 cells and was shown to promote cell death at concentrations of 30nM and 300nM *in vitro* (Figure 18). Both concentrations resulted in more than 90% of cell killing over a period of five days. B16F10 melanoma cells showed sensitivity to the microtubule poison, JG-03-14, at concentrations of 250 nM and 500 nM (Figure 19). Our studies further indicated that both stilbene 5c and JG-03-14 induce autophagy and senescence, but not apoptosis in melanoma cells (Figure 20, Figure 21). We evaluated the effect of intraperitoneal administration of stilbene 5c and JG-03-14 at non-toxic doses 25 mg/kg and 200 mg/kg, respectively. B16F10 melanoma cells were chosen for this assay due to the susceptibility of these cells to travel through the circulation and metastasize onto the lungs to form dark nodules. C57BL/6 mice were injected intravenously with B16F10 melanoma cells and mice were then treated with 25 mg/kg/day five days a week for two weeks. In this study, neither stilbene 5c nor JG-03-14 prevented the invasion of B16F10 melanoma cells into the lungs according to the number of tumor nodules ( $64.375 \pm 51.5$  with vehicle,  $83.25 \pm 55.257$  with 25 mg/kg/day stilbene 5c and  $52.125 \pm 47.7$  with 200 mg/kg/day JG-03-14; n=8) (Figure 22). We further measured the surface area of each nodule to assess whether stilbene 5c or JG-03-14 disrupts the vascular perfusion of the tumor. Lungs were sectioned at thickness of 4 microns and embedded into Eosin and Hematoxylin and nodules sizes were measured and

analyzed. While JG-03-14 induced a significant decrease of average nodule size, our calculations revealed that a non-significant reduction in tumor volume resulted from the treatment with stilbene 5c ( $0.0518 \text{ mm}^3 \pm 0.006416$  with vehicle,  $0.0403 \pm 0.00972$  with stilbene 5c, and  $0.02145 \pm 0.004113$  with JG-03-14,  $p = 0.0573$ , vehicle vs treated,  $n = 6$ ) (Figure 24).

**Figure Legends.****1.**

**Figure 1. Sensitivity of HCT116 cells to stilbene 5c.** Viability of HCT-116 colon cancer cells to stilbene 5c was measured by the MTT assay. 6000 cells were plated in 96-well plates and continuously exposed to the indicated concentrations of stilbene 5c for 72 hours. MTT dye was added to each well and cells were incubated for an additional 3 hours. DMSO was then used to dilute the precipitated MTT dye and the absorbance was read at wavelength 490 nM. This experiment was done in triplicate and error bars represent standard deviation (\*  $p < 0.05$  compared to control)



2.

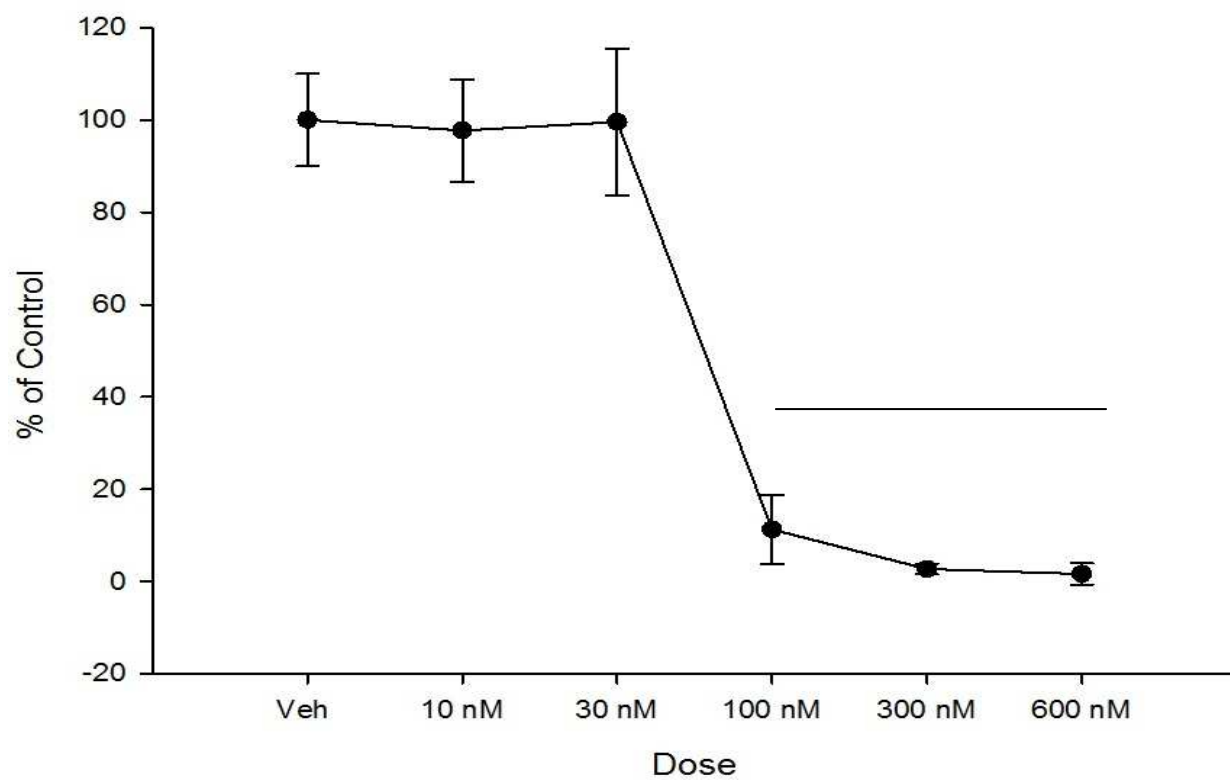


**Figure 2. Determination of sensitivity to stilbene 5c based on clonogenic survival.** HCT116 cells were plated in 6-well plates and treated with the indicated concentrations for 48 hours. Drug was washed out and cells were supplemented with fresh medium every other day for an additional 7 days. Number of colonies in each well was counted and calculated as a percentage of control. This experiment was performed in triplicate and error bars represent standard deviation (\*  $p < 0.05$  compared to control)

3.

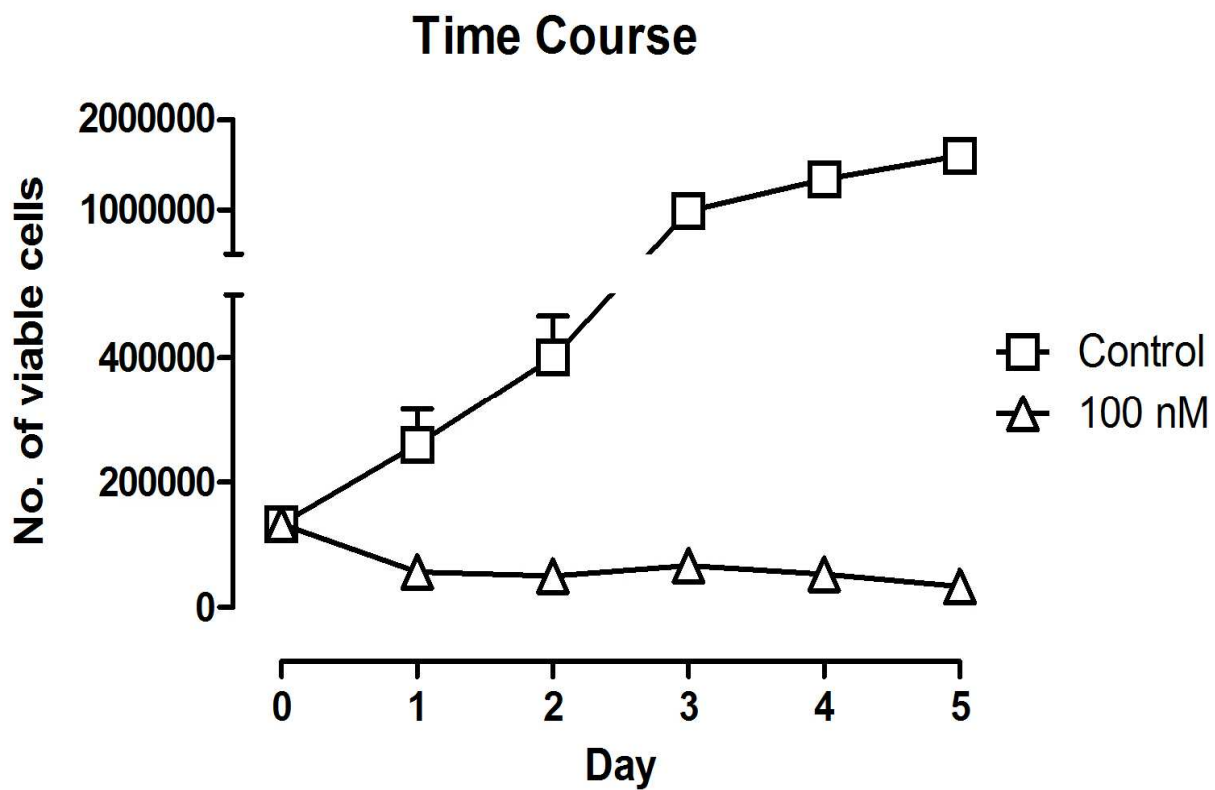
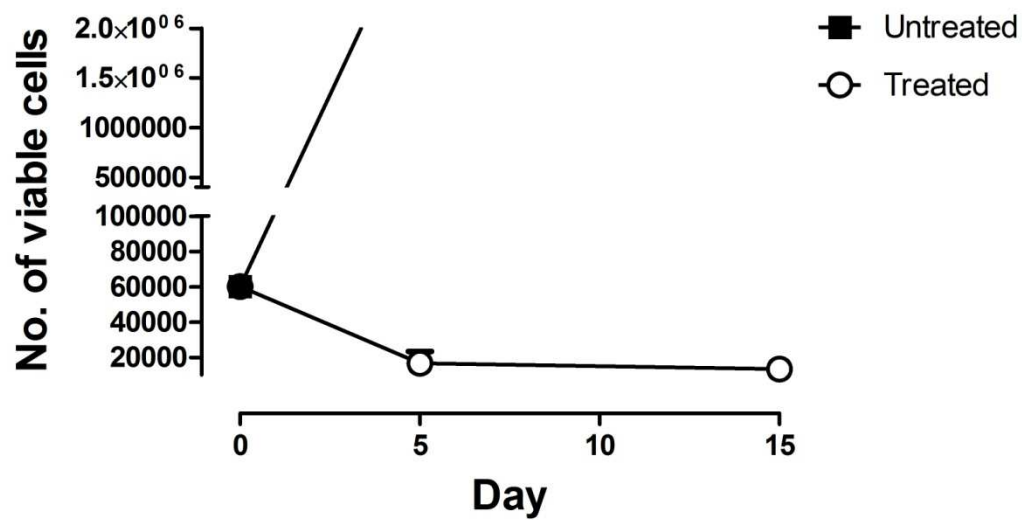


**Figure 3. Time course study of HCT116 cells after continuous exposure to 100 nM stilbene**

**5c.** HCT-116 cells were plated in 6-well plates and treated with 100 nM of stilbene 5c over a period of 5 days. Cells were harvested and collected and viable cell number was determined by trypan blue exclusion assay using the automated Countess cell counting device. Cells were plated in triplicate for each condition. This experiment was performed in different times (\*  $p < 0.05$  compared to control)

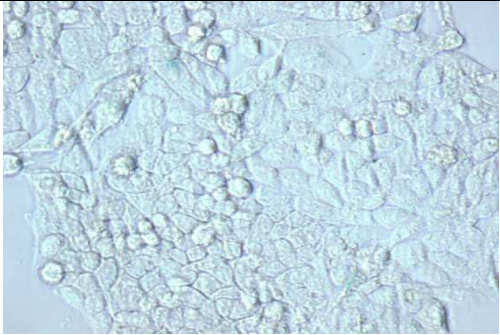
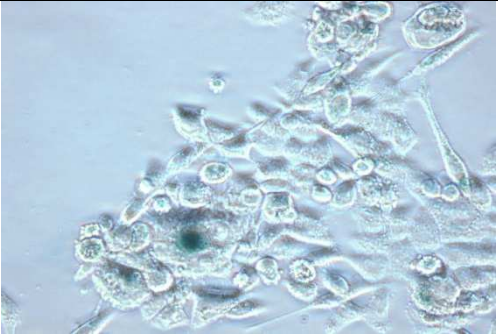
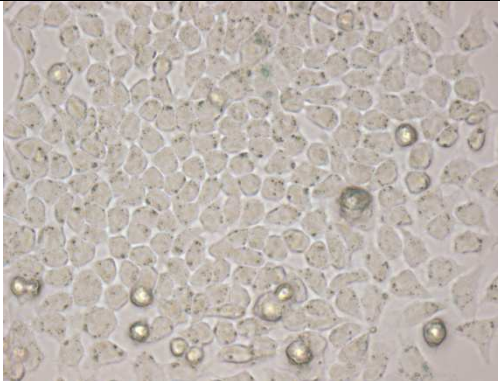
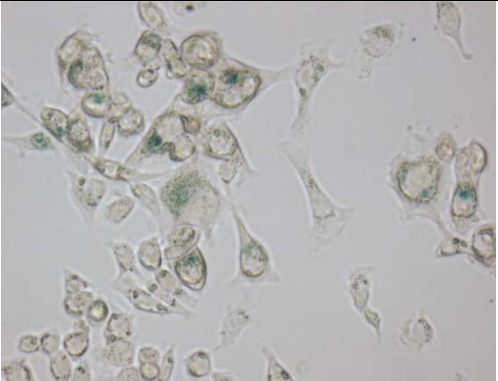
4.

### Loss of Proliferative Recovery After the exposure of 100 nM of Stilbene 5C



**Figure 4. Continuous exposure to stilbene 5c leads to loss of proliferation.** The time course study shown in figure 3 was extended for 10 more days post treatment. On day 5, the drug was removed and remaining cells were supplemented with fresh medium every other day until day 15. At indicated time points, cells were harvested with trypsin and counted using trypan blue exclusion assay. This experiment was performed in triplicate.

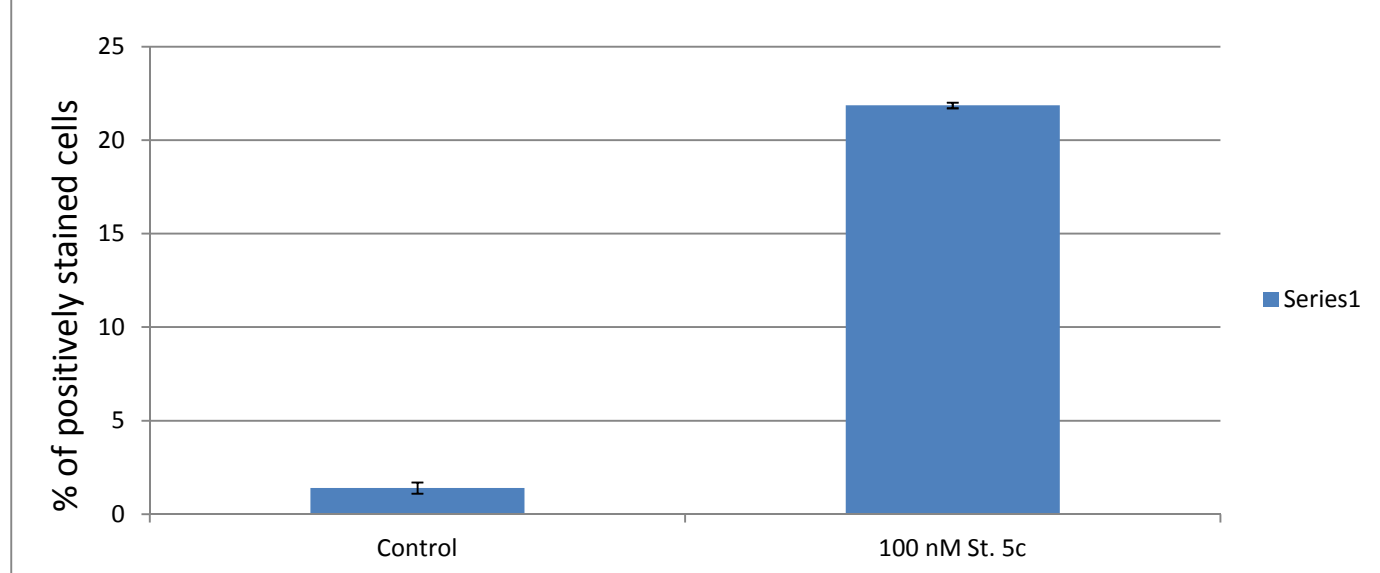
5.

	Control	100 nM St. 5c
Day 3	 Micrograph showing a dense, confluent monolayer of cells in the control group on Day 3. The cells are well-spread and cover most of the field of view.	 Micrograph showing a sparse, non-confluent monolayer of cells in the 100 nM St. 5c treated group on Day 3. There are significant gaps between the cells.
Day 4	 Micrograph showing a dense, confluent monolayer of cells in the control group on Day 4. The cells are well-spread and cover most of the field of view.	 Micrograph showing a sparse, non-confluent monolayer of cells in the 100 nM St. 5c treated group on Day 4. There are significant gaps between the cells.

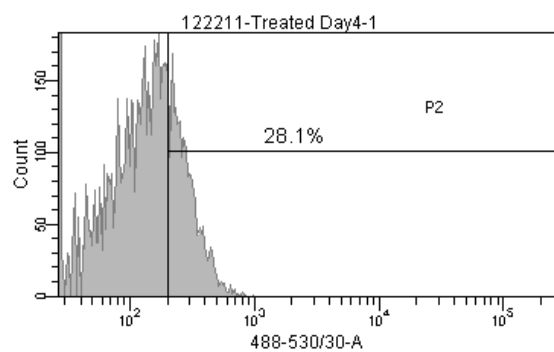
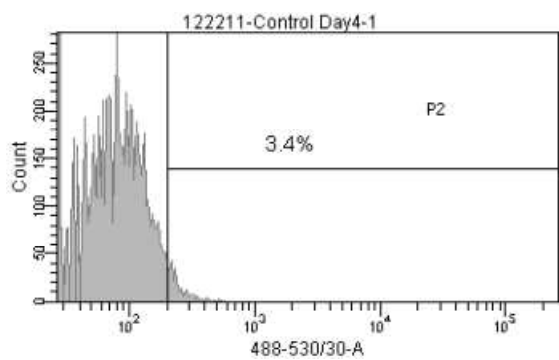
**Figure 5. Chronic treatment of 100 nM stilbene 5c promotes senescence in HCT116 colon carcinoma cells.** HCT116 cells were plated in 6-well plates and exposed to 100 nM of stilbene 5c. The drug was then removed and cells were incubated with staining buffer and X-gal for overnight. Using electron microscopy at the magnification power of 20X, the morphological markers of senescence were obvious with a remarkable increased blue color stain observed in treated cells. The result was confirmed by three different experiments.



### Evaluation of intensity of $\beta$ -Galactosidase staining in HCT-116 cells after continuous exposure to Stilbene 5c for 4 days



A.



B.

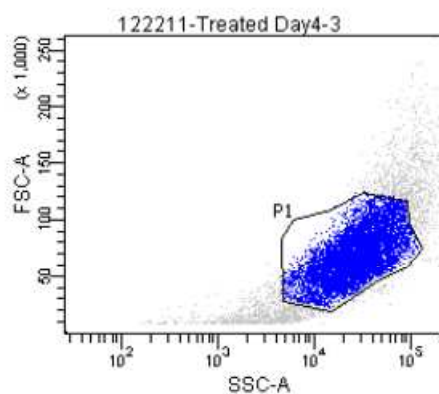
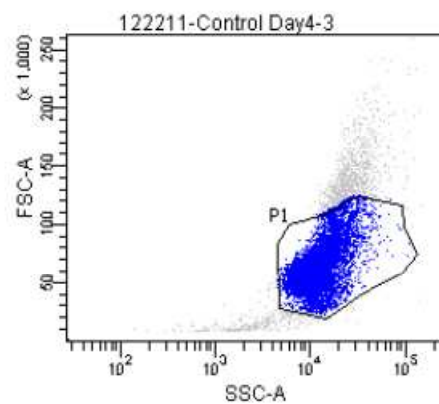
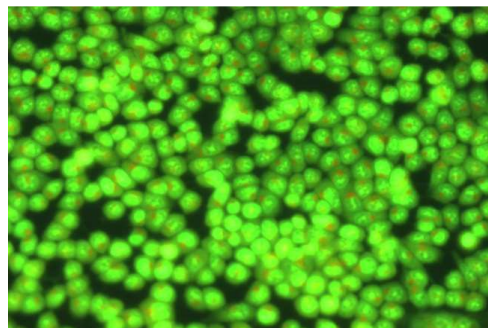
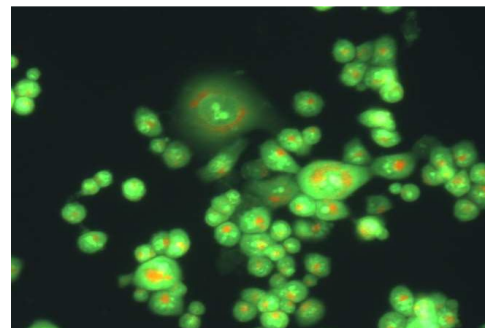


**Figure 6. Assessment of induced senescence by quantification of  $\beta$ -galactosidase staining intensity in stilbene 5c-treated HCT116 cells.** In addition to the classical microscopic method, induction of senescence could be assessed by flow cytometry to measure the fluorescence of  $\beta$ -galactosidase staining and size of cells. Data presented in the graph were generated based on the percentage of cells that were positively stained with  $\beta$ -galactosidase in both treated and non-treated conditions i.e cell population in P2 area of Panel A. In panel B, treated cells showed a rightward shift, indicating an increase in the size, complexity and granularity of treated cells. This experiment was performed in triplicate (\*  $p < 0.05$  compared to control)

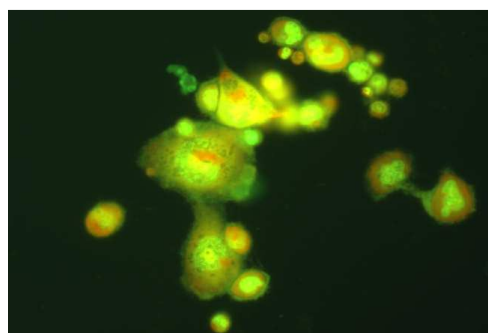
7.



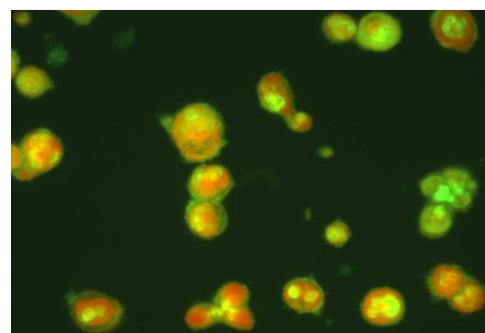
Control



Day 1



Day 2

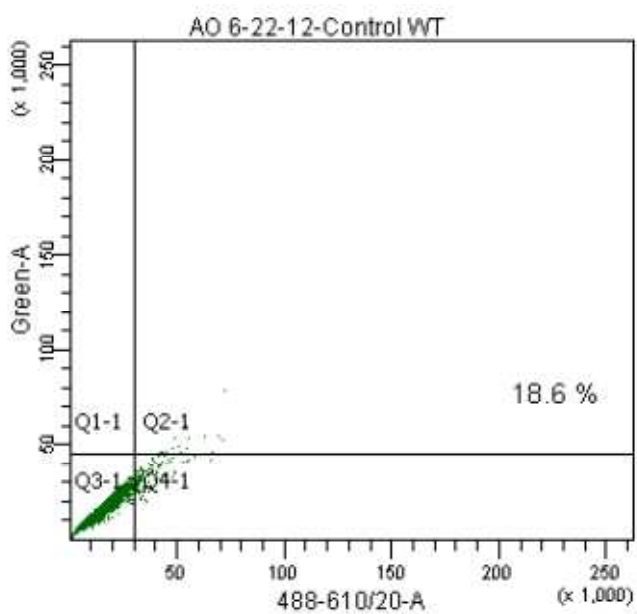


Day 3

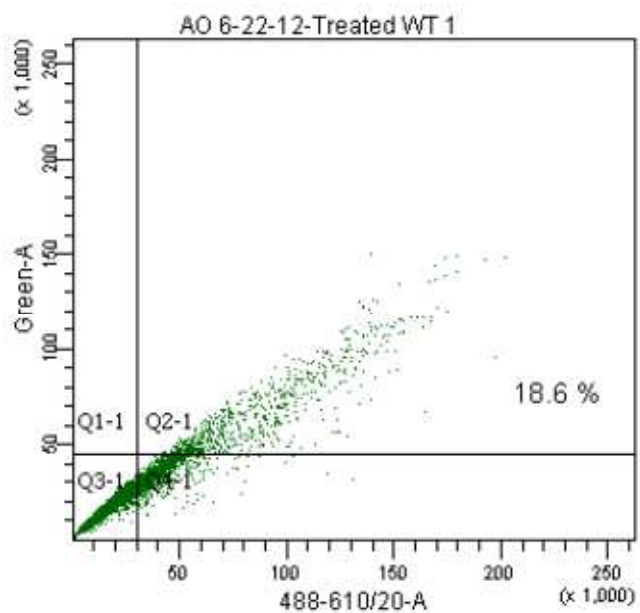
**Figure 7. Evaluation of autophagy induction by acridine orange staining.**

Cells were plated and treated with 100 nM of stilbene 5c. At indicated points, acridine orange diluted in medium in a ratio of 1:10000 was added to cells. During autophagy, acidic vacuoles are stained with acridine orange dye. Images were taken under a fluorescent microscope at a magnification power of 200X. Three different experiments were performed to confirm the result.

8.



Control



Day 3

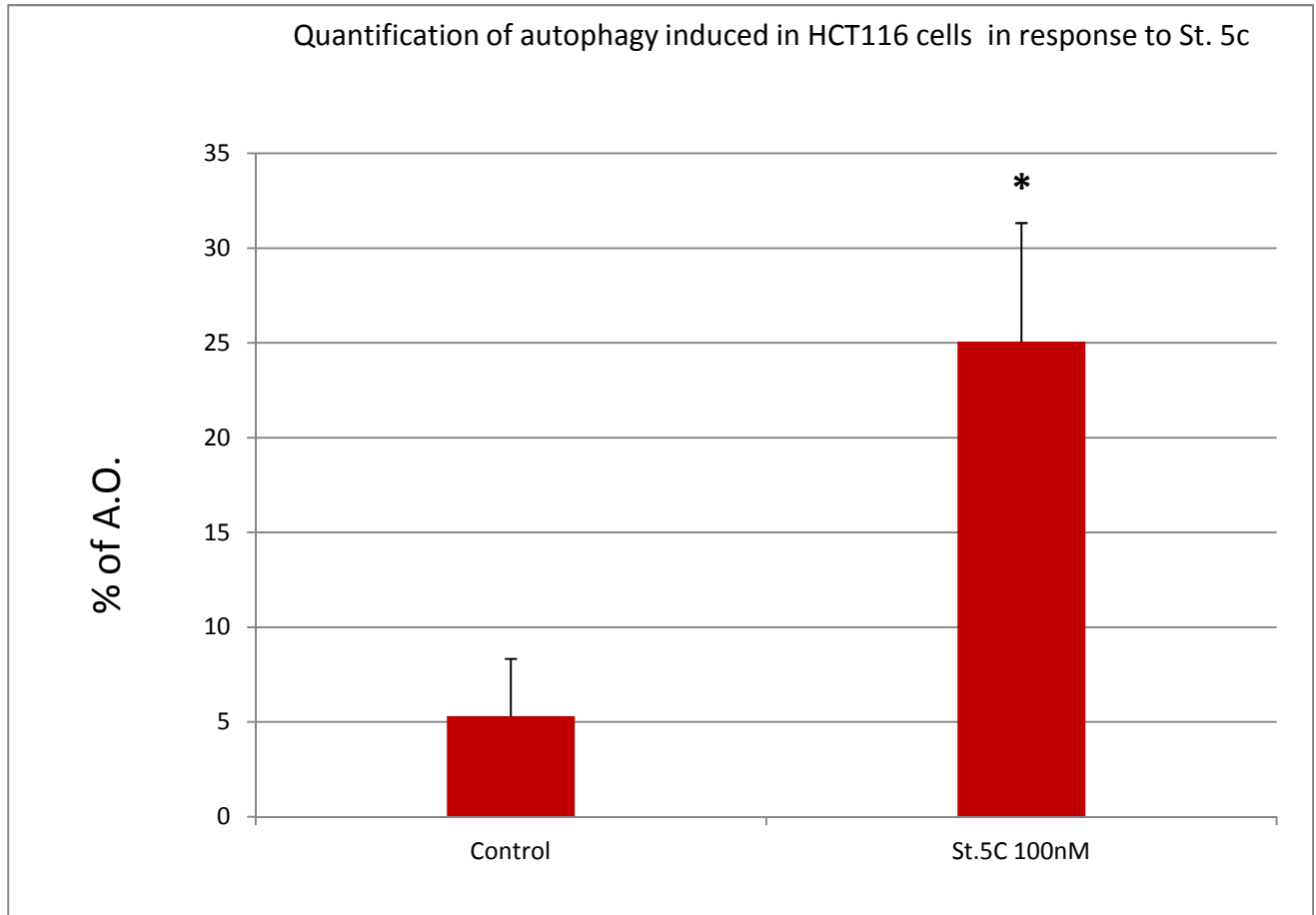
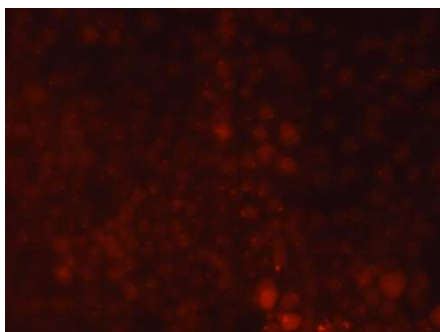
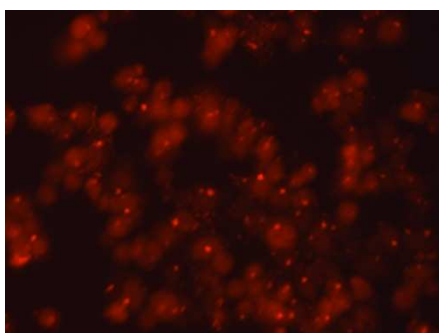


**Figure 8. Quantification of intensity of autophagy by flow cytometry.**

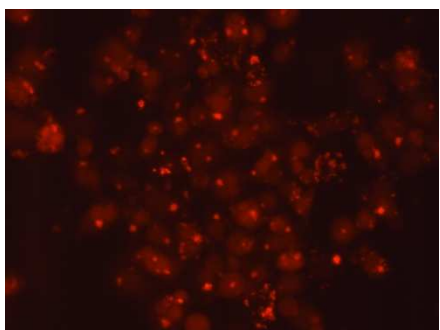
Cells were treated with 100 nM stilbene 5c for 3 days. Cells were then harvested and centrifuged at 1500 rpm. Acridine orange was diluted in PBS in a ratio of (1:10000) and was then added to the cells for staining. The extent of autophagy was counted based on the number of cell population in quadrants Q2 and Q4 from our raw data. This experiment was performed three times (\* p<0.05 compared to control)



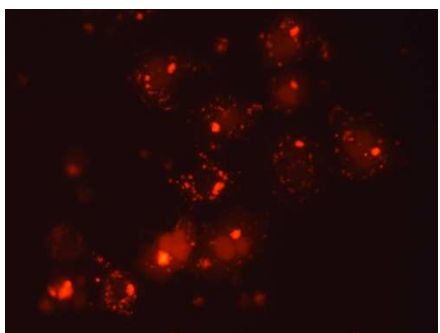
**Control**



**Day 1**



**Day 2**



**Day 3**



**Figure 9. Stilbene 5c promotes the formation of red puncta with LC3-II in RFP-LC3**

**HCT116 colon cancer cells.** HCT116 cells were transfected with an RFP-LC3 vector and plated in 6-well plates. Cells were then treated with 100 nM stilbene 5c for up to 3 days. At each time point, drug was removed and cells were washed with sterile PBS. Images were taken under a fluorescent microscope with a magnification power of 20X. Cells undergoing autophagy are characterized by increased number and size of red puncta with a remarkable enlargement of cells.

10.

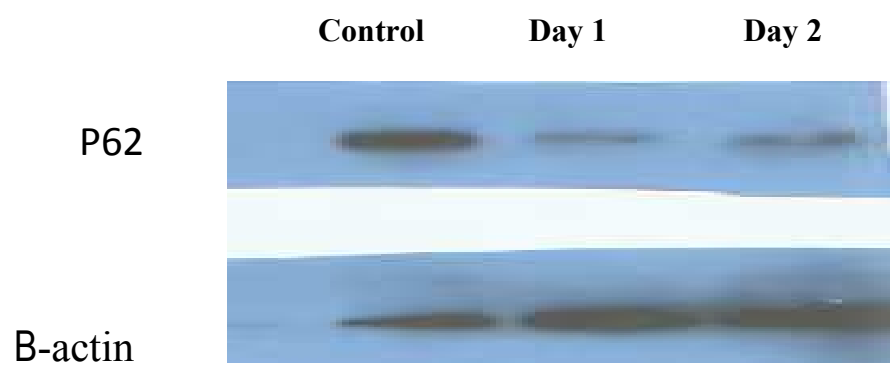


**Figure 10. Degradation of p62 protein after treatment of HCT116 cells with 100nM stilbene 5c.**

Completion of autophagy process was confirmed via the degradation of p62 by western blotting.

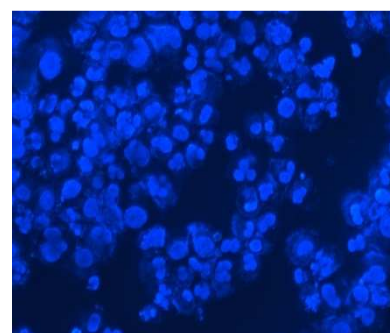
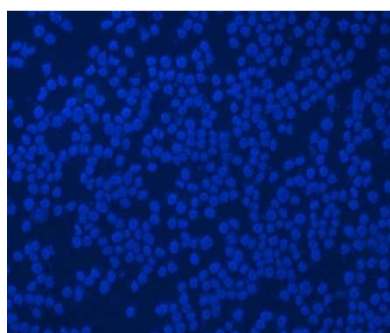
HCT116 human colon cancer cells were treated with 100nM stilbene 5c for 24 and 48 hours and levels of p62 protein was measured. A clear degradation was obvious in response to 100nM stilbene 5c.

11.

Control

100 nM St.5c (Day 3)

DAPI



TUNEL

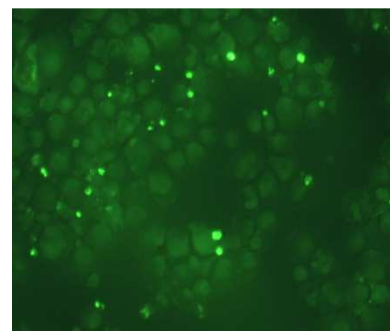
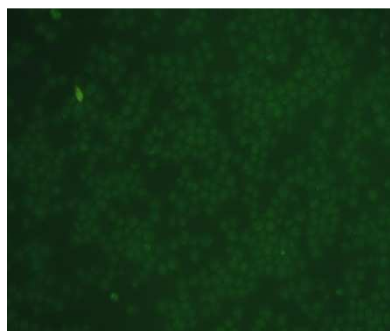
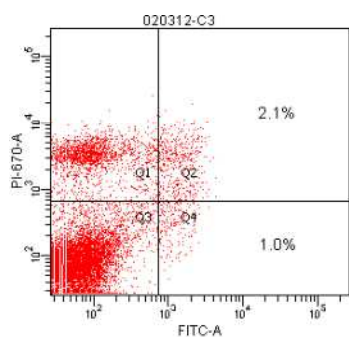


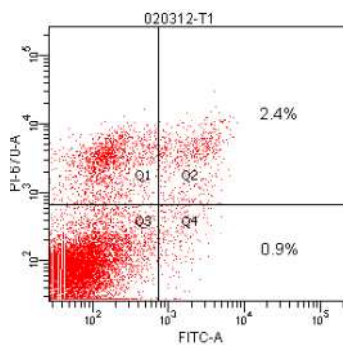
**Figure 11. Assessment of apoptosis by detection of DNA fragmentation using the TUNEL assay.**

HCT116 colon carcinoma cells were exposed to 100 nM stilbene 5c for 3 days. Cells were then loaded on slides, stained by DAPI/TUNEL, and covered by cover slips. Images were taken under a fluorescent microscope using a magnification power of 200X. DAPI stain is used to localize the nuclei in both treated and non-treated cells. The fluorescent dots represent the fragmented sites on DNA, which are considered a hallmark of apoptosis. Two different experiments were performed to confirm the result.

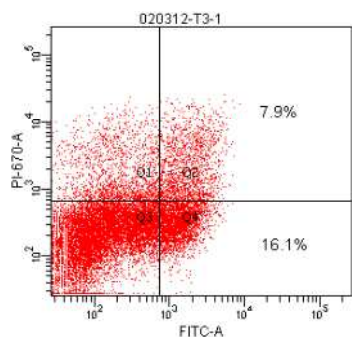
## 12. A.



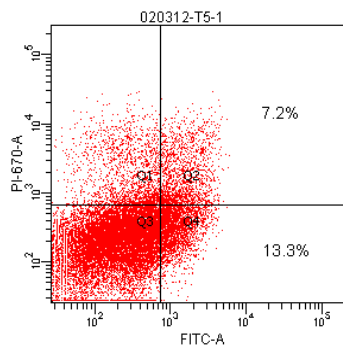
Control



Day 1

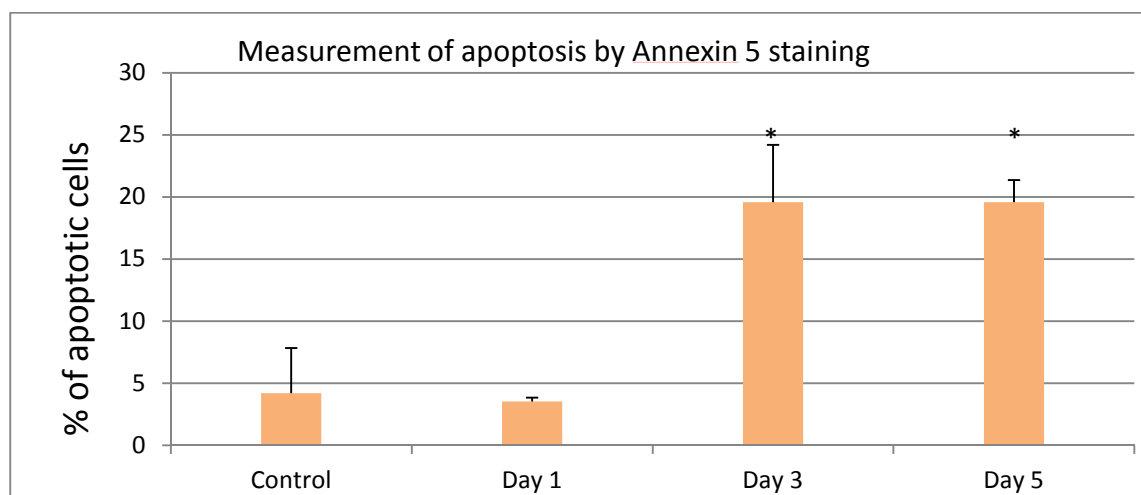


Day 3



Day 5

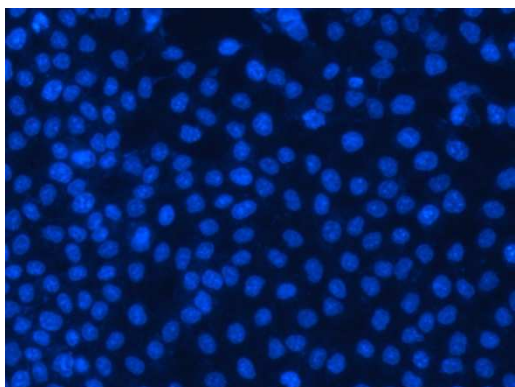
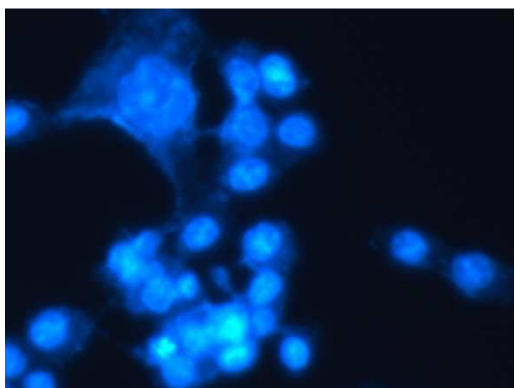
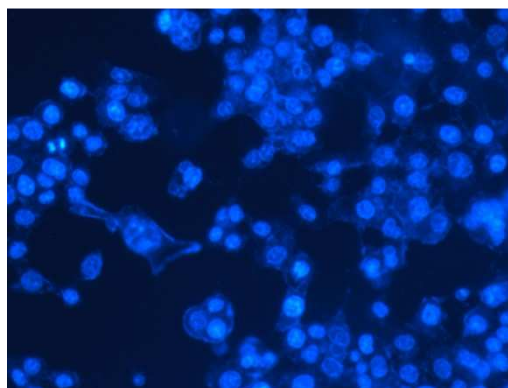
## B.



**Figure 12. Stilbene 5c induces apoptosis in HCT116 colon cancer cells.**

Cells were treated with 100 nM stilbene 5c for one, three, and five days and stained with Annexin V and PI to assess whether cells die via apoptosis and/or necrosis . The raw data show four quadrants; wherein, Q1 corresponds to necrotic cells only, Q2 reflects the late apoptotic cell population, Q3 indicates cells that neither apoptotic nor necrotic cells, and Q4 indicates early apoptosis. The percentage of apoptotic cells presented in Panel B is counted based on percentage of cells in both Q2 and Q4. This experiment was performed twice (\*  $p < 0.05$  compared to control)

13.

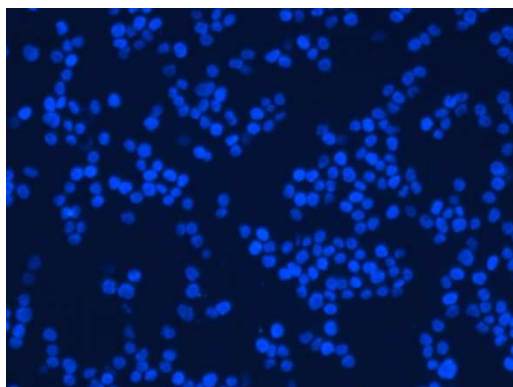
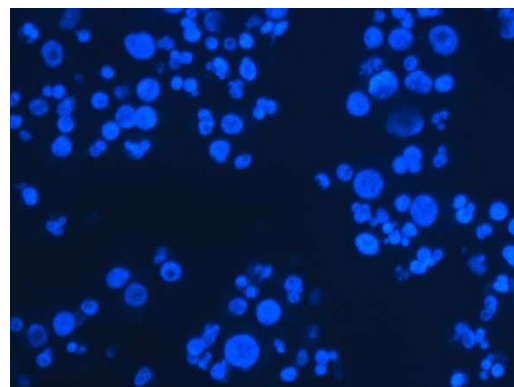
**Control****Day 1****Day 2****Day 3**



**Figure 13. Mitotic catastrophe is promoted in HCT116 cells in response to 100 nM stilbene 5c.**

HCT116 colon cancer cells were plated in 6-well plates and treated with the indicated concentration. At the indicated time points, drug was washed out and a dilution (1:10,000) of DAPI in PBS was added to stain the nuclei. Images were taken under a fluorescent microscope with magnification power of 200X. Markers of drug-induced mitotic catastrophe are characterized by bi-nucleated and micro-nucleated cells. This experiment was done in triplicate.

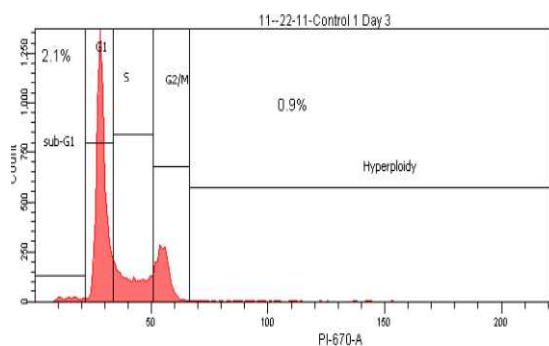
14.

**Control****St. 5c 100 nM (Day 3)**

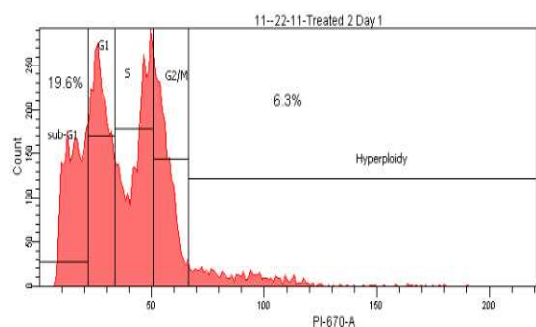
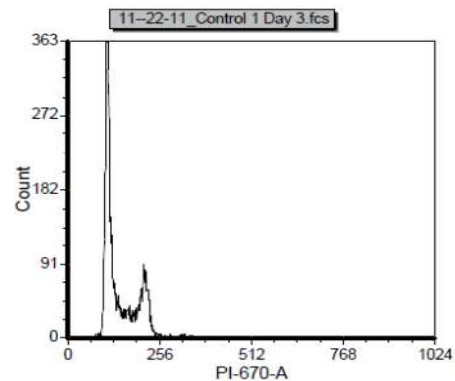
**Figure 14. Stilbene 5c – treated HCT116 cells undergo mitotic catastrophe cell death.**

Images shown in this figure represent HCT116 colon carcinoma cells treated with 100 nM stilbene 5c for three days. Cells were then collected and loaded on cover slips on which nuclei were stained with Hoechst dye. In control cells, nuclei are separated and well rounded; whereas, treated cells nuclei appear abnormal in size with more than one nucleus in the same proximity due to the failure to fall apart as well as clear bi-nucleation, indicating the induction of mitotic catastrophe. This experiment was performed twice.

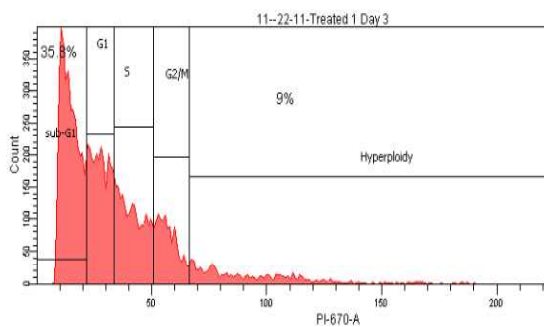
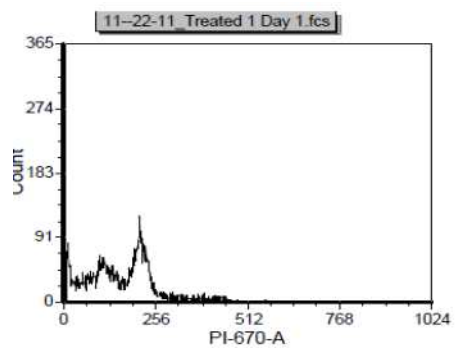
15.



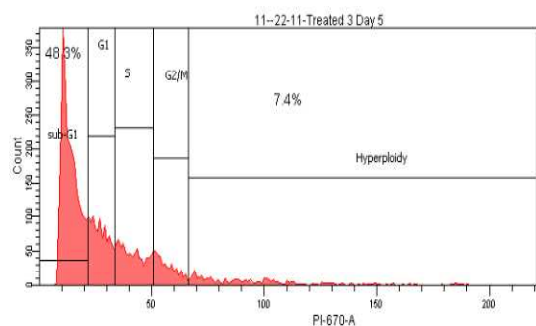
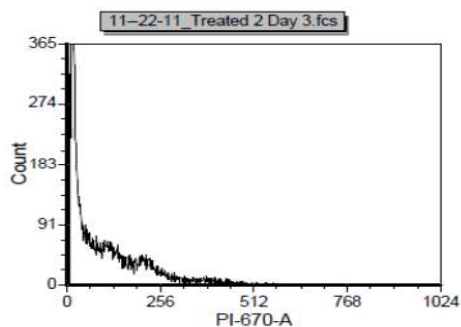
Control



Day 1



Day 3



Day 5

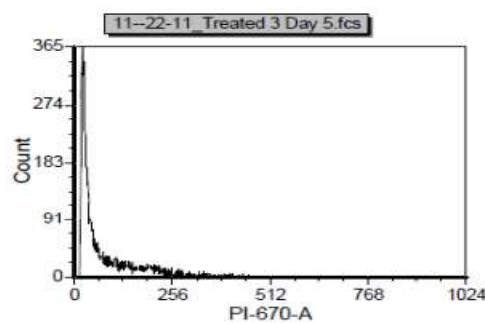


**Figure 15. Cell cycle analysis demonstrates growth and cell death in HCT116 colon cancer cells after exposure to 100 nM stilbene 5c.** Cells were plated in 6-well plates and allowed to adhere overnight. Serum-deficient medium was added overnight to synchronize the cells at the same phase. On day 0, drug was added to treatment wells and control cells were supplemented with fresh medium. At each time point, cells were trypsinized and the experiment was performed as explained in chapter 2. Cells were arrested at the G2/M phase 24 hours post-treatment with an increase in the sub-G1 population in time-dependent manner. Images in the right column show the same distribution of cells but in normalized cell count (Y) axis. This experiment was performed twice.

16.

**Time-Course Study of 100nM stilbene 5c  
on HCT-116 (p53<sup>-/-</sup>) cells**

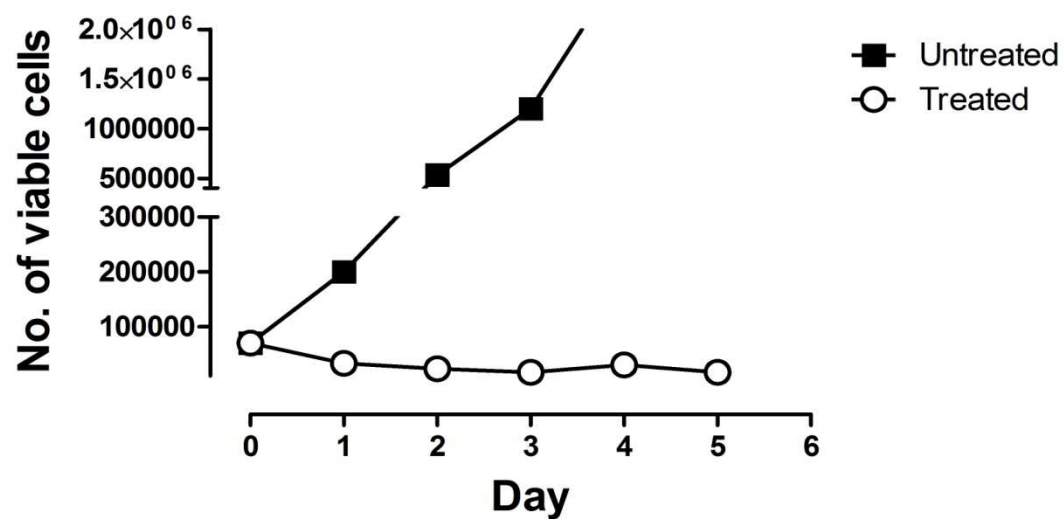


**Figure 16. Similar response of p53-null HCT116 cells and p53-wt HCT116 cells to 100 nM stilbene 5c.**

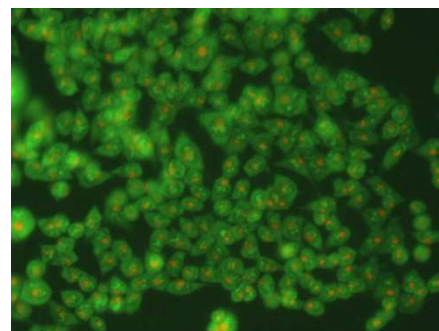
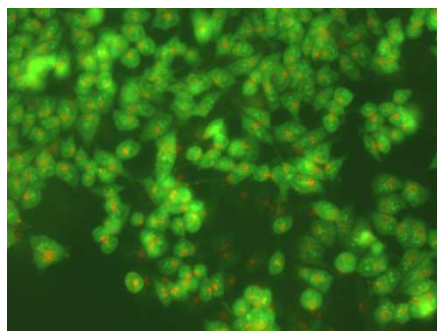
The p53-null HCT-116 cells were plated in 6-well plates and treated with 100 nM of stilbene 5c over a period of 5 days. Cells were harvested and collected and viable cell number was determined by trypan blue exclusion assay using the automated Countess cell counting device. Cells were plated in triplicate for each condition. This experiment was performed in three different times (\*  $p < 0.05$  compared to control)

17.

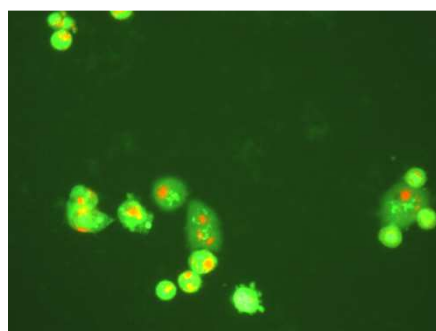
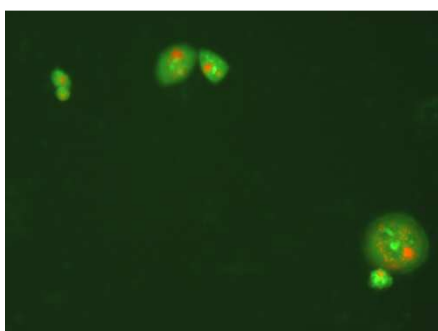
p53-wt HCT116 cells

p53-null HCT116 cells

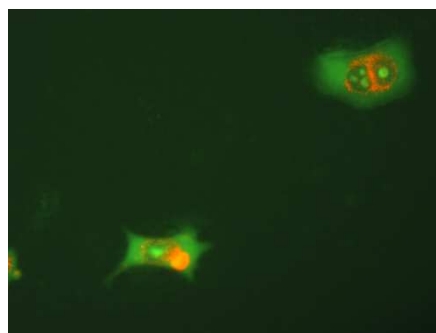
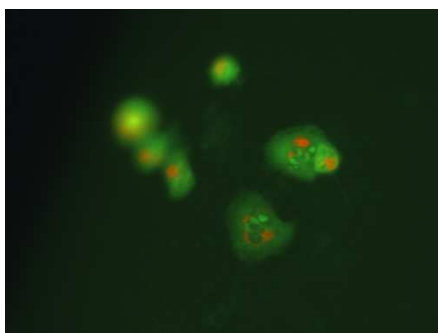
Control



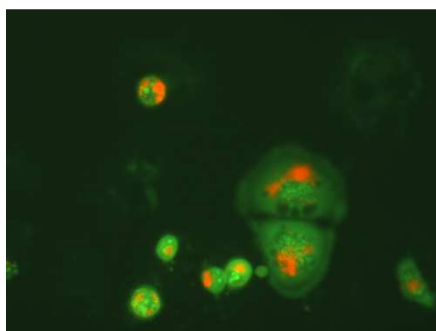
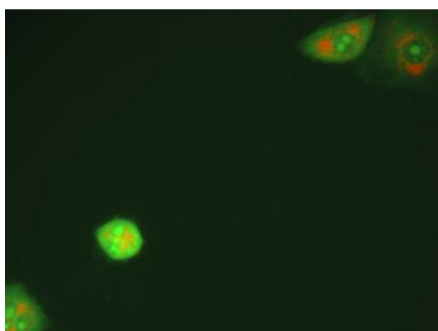
Day 1



Day 2



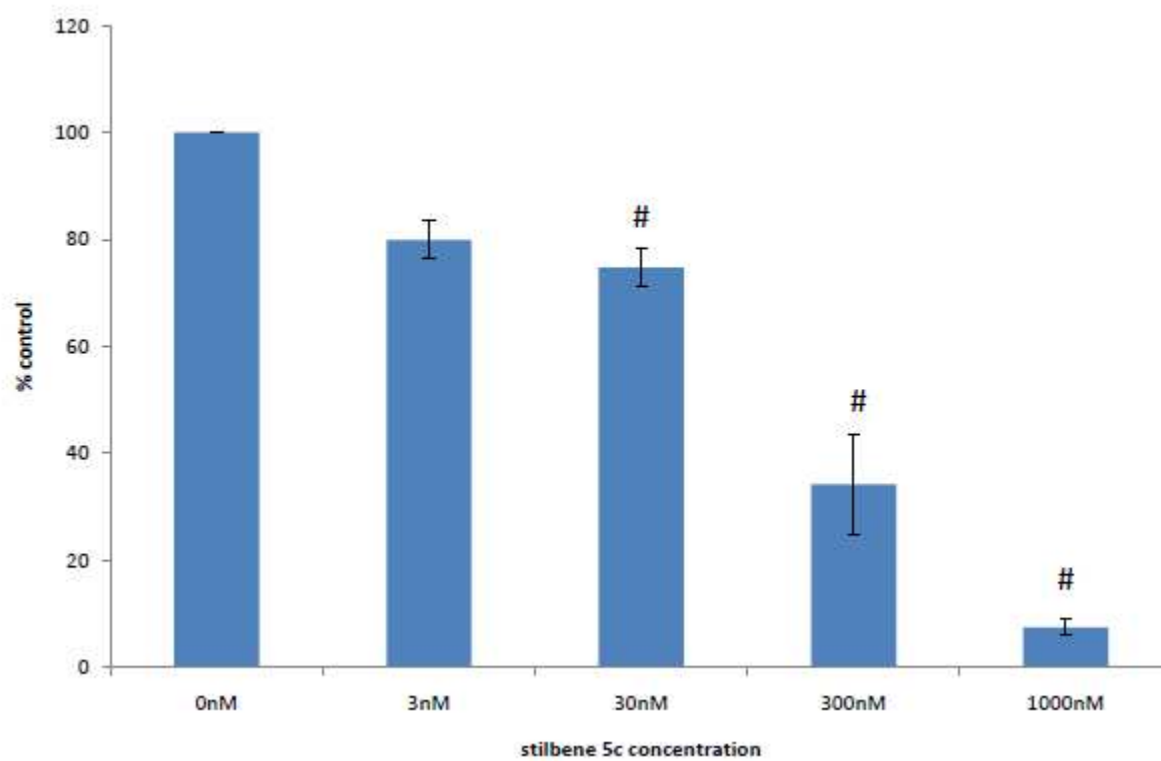
Day 3





**Figure 17. Promotion of autophagy in p53-null HCT116 colon cancer cells after exposure to 100 nM stilbene 5c.** Both p53-null and –wild type HCT116 colon cancer cells were plated in 6-well plates and treated with 100 nM stilbene 5c. At indicated time points, drug was removed and cells were stained with acridine orange for 15 minutes. Images were taken under a fluorescent microscope at magnification power of 20X. This experiment was performed in triplicate.

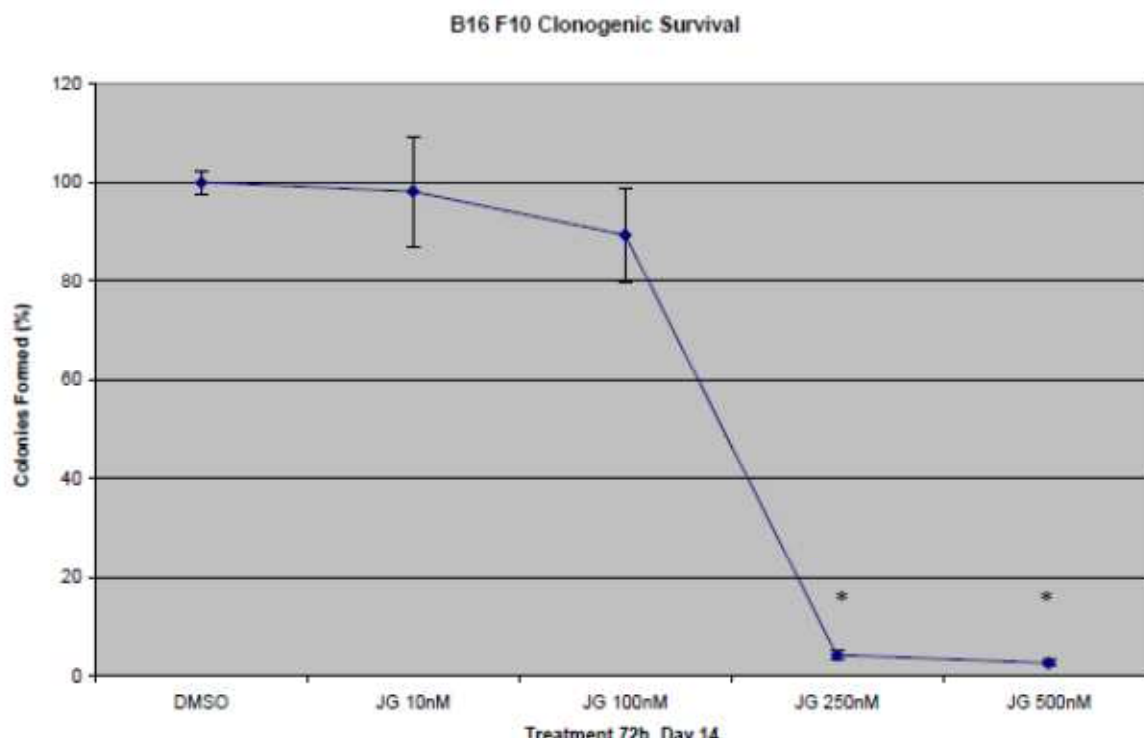
18.



**Figure 18. Inhibition of colony formation in B16F10 melanoma cells by stilbene 5c.**

150 cells of B16F10 cells were plated per well in triplicate in 6 well plates. Control cells were seeded at the same density and allowed to incubate in drug free medium while cells treated with 3nM, 30nM, 300nM and 1000nM stilbene 5c were incubated for 72 hours. Drug containing medium was removed at the end of the 72 hours and replaced with fresh medium. When colonies of at least 50 cells are visible to the naked eye, cells were stained with crystal violet and counted visually. The number of colonies formed decreased in a dose-dependent manner in cells treated with stilbene 5c compared to control cells. (#  $p < 0.05$  compared to control)

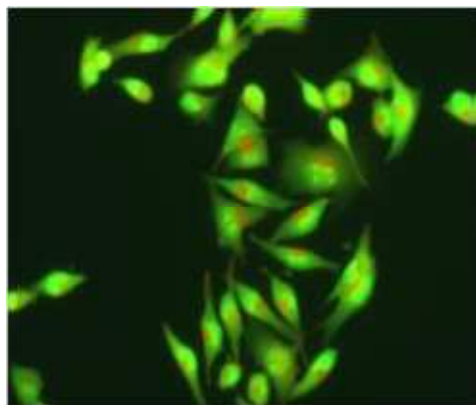
19.



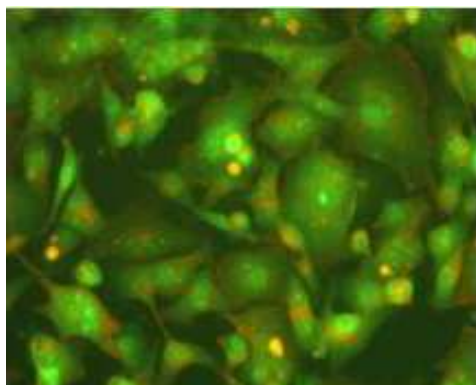
**Figure 19. A dose-dependent decrease in colony formation in B16F10 in response to JG-03-14.**

B16F10 cells were plated at a density of 100 cells/plate for DMSO, JG 10 nM and 500 cells/plate for JG 250 nM and JG 500 nM. Assay shown is a representative experiment performed in triplicate that was corrected for plating efficiency. Two identical replicate experiments were performed for confirmation. Error bars represent standard deviations and significant differences from DMSO treatment are indicated by \* ( $P < 0.05$ )

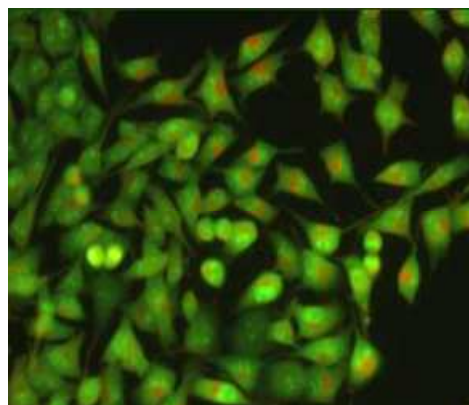
20.

**Stilbene 5c 300 nM**

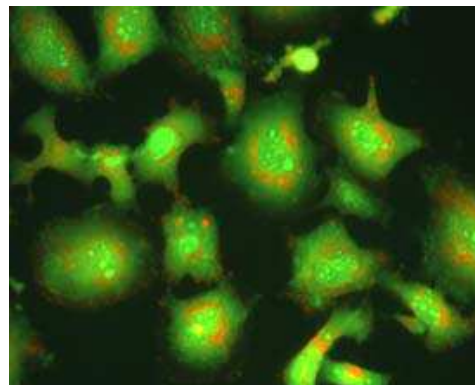
Control



Day 3

**JG-03-14 500 nM**

Control

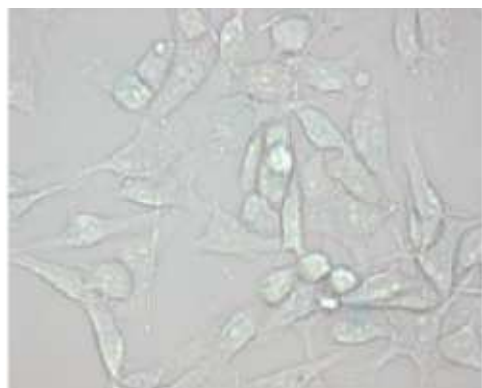


Day 3

**Figure 20. Stilbene 5c and JG-03-14 induce extensive autophagy in B16F10 melanoma cells.**

Acridine Orange staining was utilized to assess the induction of autophagy in B16F10 cells treated with 300nM stilbene 5c and 500nM JG-03-14. Cells were plated, incubated overnight and treated the following day with either 300nM stilbene 5c or 500nM JG-03-14. Acridine Orange images were taken using an inverted fluorescent microscope. Induction of autophagy was apparent due to the orange puncta distribution in the treated cells.

21.

**Stilbene 5c 300 nM (Day 3)**

Control



Day 3

**JG-03-14 500 nM (Day 3)**

Control



Day 3



**Figure 21. JG-03-14 and stilbene 5c promote senescence in B16F10 melanoma cells.**

B16F10 cells were treated with 500nM JG-03-14 and 300 nM stilbene 5c for 72 hours in two individual studies. Drug was washed out and cells were stained with  $\beta$ -galactosidase as a marker of senescence. Images were taken at the magnification power of 200X.

22.

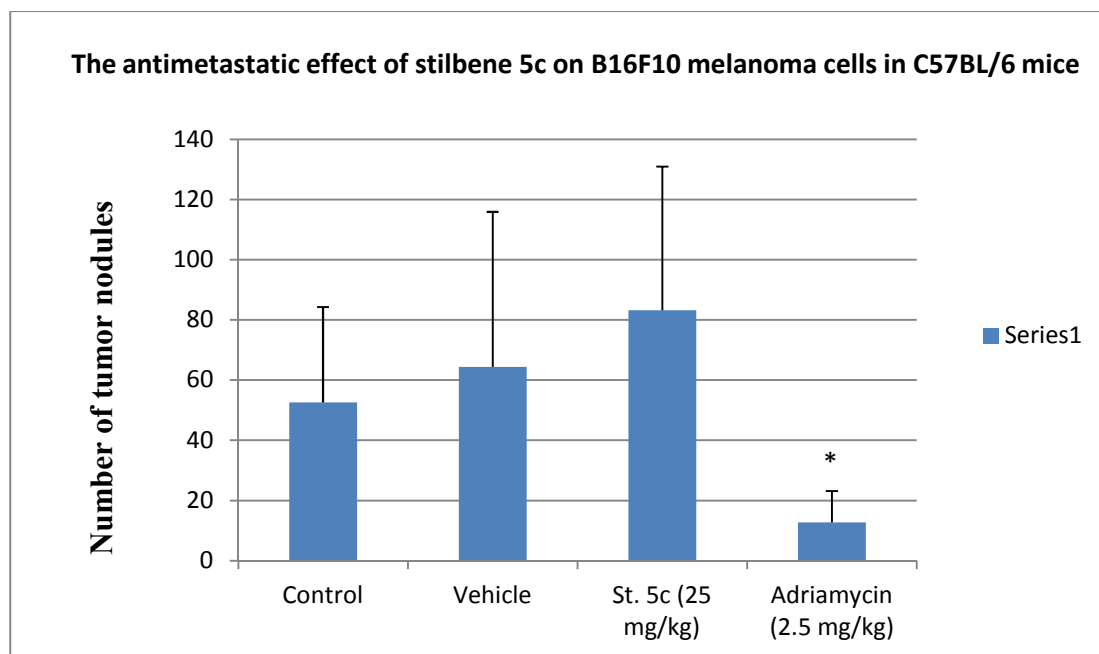
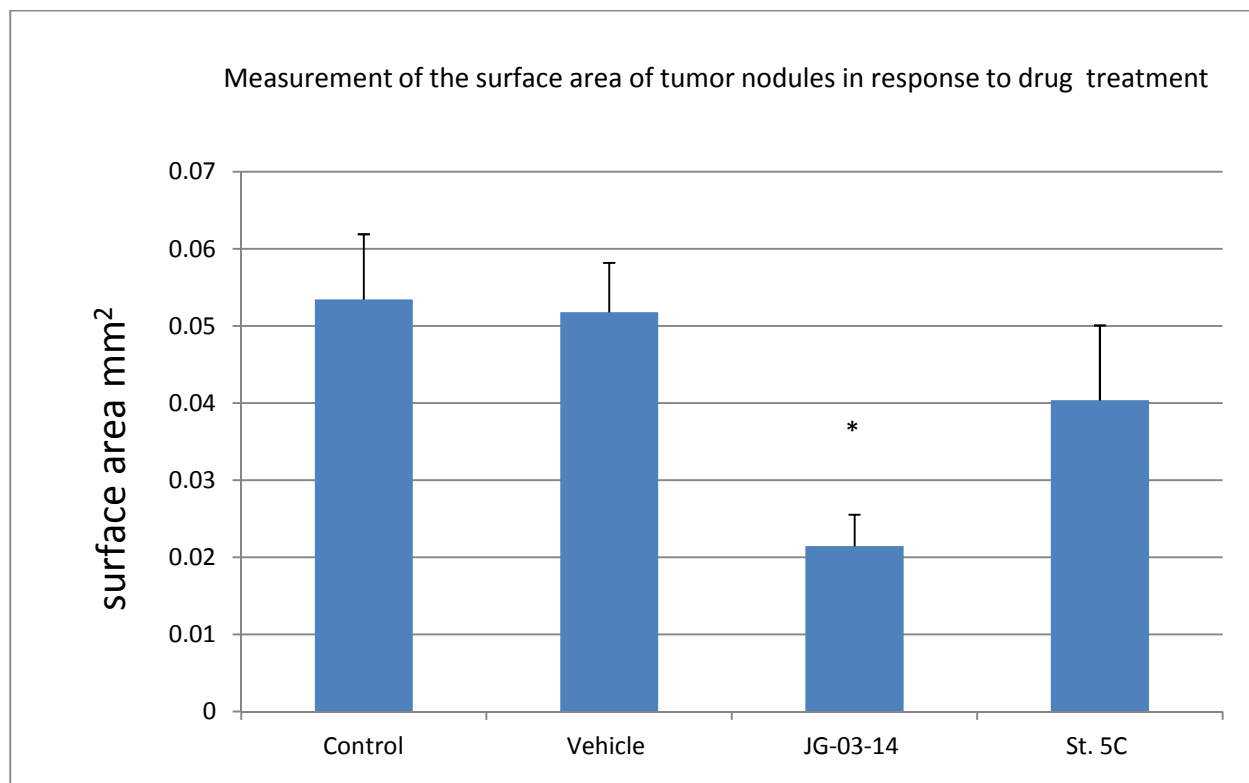


**Figure 22. Stilbene 5c did not suppress the metastasis of B16F10 melanoma cells in C57BL/6 mice.**

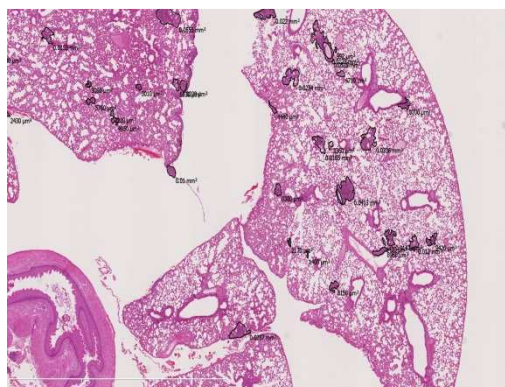
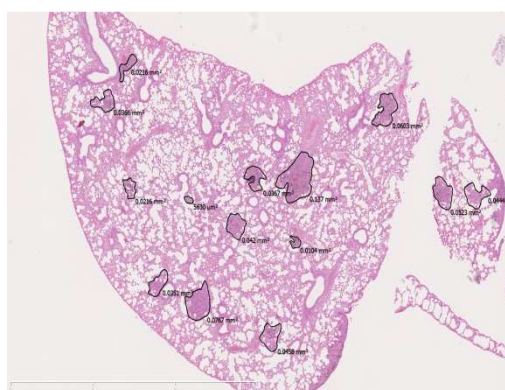
B16F10 melanoma cells that are syngeneic in C57BL/6 mice were injected intravenously. Drug was administered intraperitoneally once per day for five days a week over a period of two weeks. The vehicle used was a mixture of ethanol, tween and saline in a ratio of 2:1:7. Adriamycin was used as a positive control. The efficacy of drug was measured according to the number of dark nodules metastasized to the lungs. (\*  $p < 0.05$  compared to control,  $n = 8$ )

23.



**23. Evaluation of the effect of stilbene 5c on tumor growth and vascular perfusion.** The surface area of each nodule was measured by staining the tumor nodules with Hoechst stain. Images of the nodules were taken microscopically and nanozoomer computer software (Olympus) was used to measure the surface area of each nodule. The average nodule size was calculated per mouse for six mice per each group. Non-significant reductions in the surface area were induced by stilbene 5c.

24.

**Vehicle****JG-03-14 (200 mg/kg/day)****St. 5c (25 mg/kg/day)**

**Figure 24. Images of B16F10 tumor nodules metastasized to mice lungs.** Lung tissues were paraffin embedded, sectioned at 4 microns thickness and stained with Hematoxylin and Eosin. Tumor nodules appear darker when stained with 1H&E. Also, dark nodules are considered cancerous as they show melanin pigments and abnormal nuclear shape when they were observed by nanozoomer computer software.

## Chapter 4: Discussion

### 4.1 Overview

Microtubules are dynamic proteins that play major functions in trafficking, signaling, division, and migration in eukaryotic and mammalian cells. These proteins are found in both interphase and dividing cells. Therefore, many microtubules inhibitors were developed and evaluated for their activity against multiple diseases such as malaria and cancer [78].

Different microtubule poisons have been utilized to treat various forms of cancer. The mechanism of microtubule poisons' action is thought to be by the alteration of microtubule dynamics. Vinca- and Colchicine-binding inhibitors destabilize microtubule depolymerization; while, taxanes increase polymerization at high doses. Vinca alkaloids and taxanes were discovered more than 40 years ago and have been used effectively in the treatment of different solid and haematological malignancies [79-81]. However, many colchicine-binding inhibitors have been screened in vitro, in vivo, and in clinical trials, but none of them has been clinically approved for any therapeutic indication yet due to their severe neuro- and cardiotoxicities [14]. Moreover, microtubule inhibitors appear to be active in disrupting tumor perfusion. These agents target tumor vascularization by the inhibition of proliferation and migration, key role functions of microtubule, of newly formed endothelial cells. Resistance to these agents can be developed by numerous mechanisms including cellular efflux of the drug, alterations at the binding site of the drug, and inability to induce apoptosis in treated cells. Previous studies of stilbene 5c showed this drug disrupts tumor perfusion without affecting normal organ perfusion, leading to decrease of blood and oxygen to tumor cells [16]. Also, stilbene 5c was found to promote apoptosis in ovarian and leukemic cancer cells in vitro. [14-15]. In this study, we sought to evaluate the anticancer properties of stilbene 5c on HCT116 colon carcinoma cells and investigate induced modes of cell death.



#### 4.2 Cell death

Initial experiments were designed to identify effective concentrations of stilbene 5c in HCT116 cells. Cells were treated with 10nM, 30nM, 100nM, 300nM, and 600nM of stilbene 5c. According to our observations in clonogenic survival assay, 100nM stilbene 5c reduced the number of colonies formed by 90%. This concentration of stilbene also induces cell death in HCT116 cells based on a reduction in cell viability of approximately 75%. In both experiments, neither 10nM nor 30nM affected cellular proliferation or the number of colonies formed after the treatment compared to controls. This finding suggests that lower concentrations of stilbene 5c are not sufficient to inhibit colchicine-binding site on tubulin.

HCT-116 cells were treated with 100nM stilbene 5c in order to understand the behavior of HCT116 cells post-treatment in a time course study. A time dependent decrease in cell viability was observed starting within 24 hours after treatment. Two days post-treatment, the remaining live cells underwent prolonged growth arrest for the remaining time course of the study. The failure of re-growth appears to be irreversible due to the incapability of treated cells to reproduce after drug removal. This state of growth arrest demonstrates consistency with clonogenic survival assay findings, which might indicate that cells respond to stilbene 5c by undergoing senescence after cell death.

#### 4.3 Apoptosis

Previous studies of stilbene 5c in leukemia and ovarian cancer *in vitro* models revealed that cells die primarily through apoptosis [14-15]. As shown by time course study, extensive cell death occurs early after the exposure of HCT116 colon cancer cells to stilbene 5c. We have mentioned earlier that the deficiency in apoptotic signaling pathways can lead to the development of resistance to microtubule poisons. HCT116 colon cancer cells have a wild-type p53 protein and proficient caspase enzymes. All of

these facts indicated that it was of importance to investigate whether apoptosis represents a primary mode of cell death. While there was no evidence of apoptosis within 24 hours post treatment, treated cells clearly showed an increase in apoptosis by 25% after 72 hours of exposure to the drug. This finding was confirmed by the TUNEL assay, where many nuclei had fragmented DNA. To further understand if the wild-type p53 plays a key role in the triggering of apoptosis in HCT116 cells in response to stilbene 5c, we treated HCT116 p53 (-/-) cells, in which apoptosis signaling pathways activation are less likely to be induced, with the drug and monitored cell viability over a period of 5 days. The p53-knock out cells responded similarly to stilbene 5c, suggesting that apoptosis is not primarily induced upon exposure to the drug. However, p53-mediated apoptosis is triggered by DNA damaging agents [82], and the previous studies of stilbene 5c revealed that this drug does not have DNA damaging properties [14]. Thus, we conclude that stilbene 5c induces cell death in a p53-independent manner and that there are modes of cell death other than apoptosis induced in stilbene 5c-treated HCT116 cells.

#### *4.4 Mitotic catastrophe*

Several antitumor agents, including microtubule poisons, can trigger mitotic spindle check points [83]. It has been shown that anti-microtubule agents induce mitotic arrest-associated cell death [84-85]. For instance, combretastatin A4, a colchicine-binding inhibitor, was found to promote a phenomenon of cell death related to mitotic catastrophe [86]. One of the interesting findings of previous stilbene 5c studies was that Chk2 deficient cells become more sensitive to stilbene 5c [14]. Some studies in the literature pointed out that activation of Chk2 proteins prevents the cell from entering the cycle by down-regulating Cdc2/cyclin B complex [87]. According to this inhibitory effect of this protein, it is speculated that mitotic catastrophe can be negatively regulated by Chk2. Treatment of Hela cells with debromohymenialdisine (DBH), a chemical inhibitor of Chk2, led to the promotion of mitotic catastrophe associated with markers of apoptosis [65]. In our study, we found that some cells failed to

complete the process of cytokinesis when stained with DAPI. This observation appears consistent with the previous findings of the cytotoxic effect of stilbene 5c on ovarian cancer cells [14]. Also, Hoechst staining confirmed that prolonged treatment of HCT116 cells results in frequent multiple micronuclei, a hallmark of mitotic catastrophe. These observations may indicate that the early seen cell death is generally not due to apoptosis, but rather through mitotic catastrophe. However, recent reports have shown that mitotic catastrophe characterizes another form of apoptosis [65, 77]. Other reports indicated that apoptosis becomes initiated after the slippage of cells from mitotic catastrophe [84, 88]. Moreover, several *in vivo* and *in vitro* studies have indicated that mitotic catastrophe is associated with the release of pro-apoptotic proteins and activation of caspases, which suggests that induction of mitotic catastrophe requires some pathways involved in mechanisms of apoptosis [64-66] This might explain why markers of apoptosis appear three days after the treatment with stilbene 5c.

Treatment of p53-null HCT116 cells resulted in a decrease in cell viability to an extent similar to that observed in the wild type p53 HCT116 cells. Some reports have argued that the p53 gene is required to induce apoptosis or senescence, but not the mitotic catastrophe [71]. Moreover, it has been thought that cells lacking functional p53 protein undergo forms of cell death rather than apoptosis such as mitotic catastrophe and necrosis [63]. Taken together, we conclude that HCT116 cells may primarily undergo mitotic catastrophe in response to the treatment with stilbene 5c. As a result, apoptosis appears after the promotion of mitotic catastrophe due to the cross-talk between these processes.

#### 4.5 Induction of autophagy

Autophagy is a catabolic process in which the cell's contents are broken down by lysosomal degradation. It is established that HCT116 colon carcinoma cells have constitutively active PI3K and *ras*

mutant genes [89]. A study by Gou *et al* proved that cells with a mutated *ras* gene, including HCT116 cells, require autophagy to survive [71]. Thus, HCT116 cells have a relatively high basal level of autophagy. Until today, it is still ambiguous what amount of autophagy is needed to induce cell death. Also, it is still indistinguishable what signaling elements are responsible for the promotion of autophagic cell death rather than cytoprotective autophagy. One of the suggested mechanisms by which autophagy becomes initiated is through the interaction with microtubules. Although the function of microtubules in the induction of autophagy is not well understood, some studies have shown that microtubules play a role in autophagosomal formation [90]. The same study demonstrated that autophagosomal level was increased by more than two fold when cells were treated with vinblastine [84]. In contrast, drugs stabilizing microtubule polymerization, such as paclitaxel, failed to increase acidic vacuoles. These results may indicate that microtubules are not essential for autophagosome development, but at least can contribute to the increase of amount of autophagosomes. Our observations suggest that the obvious increase in the amount of acidic vacuoles in response to stilbene 5c may be due to its effects on microtubule dynamics.

Induction of autophagy was confirmed by monitoring microtubule associated protein light chain LC3 expression in HCT116 cells. LC3-II, a marker of autophagy, is produced by proteolytic cleavage of LC3-I, and required for the formation of autophagosomes [91]. We found that stilbene 5c increased the number of RFP punctate pattern in treated cells as early as day 1 compared to control. This finding supports the idea that autophagy is initiated earlier than other modes of cell death. More importantly, acridine orange and RFP-LC3 transfection only indicate the induction of autophagy but not the completion of this process. Thus, another experimental technique has been used as an indicator for autophagic flux. We have monitored the level of p62 after the incubation of HCT116 cells with stilbene

5c as early as day 1. We found a clear degradation of p62 after the treatment, indicating that autophagy has been going to completion.

A recent study showed that curcumin induces autophagy in HCT116 cells in both p53-wild type and p53-deficient HCT116 cells [92]. Consistent with this finding, we have found that p53-null HCT116 cells incubated with stilbene 5c expressed a similar extent of autophagy as the p53-wild type HCT116 cells. This result strongly suggests that stilbene 5c promotes autophagy in a p53-independent manner, and may also lead to autophagic cell death.

Although the cross-talk between autophagy and apoptosis is not very well understood, an interaction between apoptosis and autophagy has been illustrated by many studies. A study by Ding *et al* indicating that Bax-positive HCT116 cells undergo autophagic cell death followed by apoptosis [93]. In the same study, it was found that inhibition of autophagy led to apoptosis in Bax-proficient HCT116 cells but not the Bax-deficient HCT116 cells, indicating that presence of Bax is important for switching the mode of cell death to apoptosis. Another study by Yousefi *et al* demonstrated that the overexpression of the ATG5 gene in human cancer cells enhances their sensitivity to undergo autophagic cell death followed by apoptosis when treated with ceramide or DNA-damaging agents [94]. In this study, when the ATG5 gene was knocked out, the susceptibility of these cells to die through autophagy was eliminated with a significant reduction in apoptotic markers. This linkage between autophagy and apoptosis can possibly be due to the cleavage of ATG5. When the cell becomes exposed to excessive autophagic stress, calpain proteins cleave ATG5 to produce a fragment that loses its autophagy-promoting activity and gains its pro-apoptotic activity [94]. This released fragment translocates into the mitochondria, where it binds to BCL-XL proteins and promote apoptosis. Also, there is another mechanism by which the ATG5 protein switches mode of cell death from autophagy to apoptosis. ATG5

gene can bind to FADD (Fas-associated via death domain) via its C terminus, which in turn stimulates caspase-dependent apoptosis [95].

In our results, we found that apoptosis was preceded by induction of both autophagy and mitotic catastrophe. We have discussed the possibility of how mitotic catastrophe leads to the induction of apoptosis. Here, we show another possibility where triggered autophagy can eventually lead to apoptotic cell death. For this reason, we expect that autophagy has the capacity to be cytotoxic in this system more than being cytoprotective. This finding can be of clinical utility, since some tumor cells have the ability to evade apoptosis, thereby showing resistance to the currently used therapeutics [41, 82].

#### 4.6 Senescence

Several studies have shown that induction of autophagy is associated with promotion of senescence in cancer cells [74, 92]. Lu *et al* found that autophagic cell death led to growth arrest in a xenograft model of ovarian cancer cells [96]. Also, the inhibition of autophagy was found to delay, but not completely inhibit, the induction of cellular senescence after exposure to an antitumor agent [70, 89]. It appears that autophagy plays a dual role either to induce senescence or promote apoptosis in response to the treatment with stilbene 5c. Due to this linkage between both these phenomena, we anticipate that the promotion of autophagy in stilbene 5c-treated HCT116 cells may lead cells to transit into senescence. Our time course treatment studies showed that treated cells apparently undergo a state of growth arrest initiated two days post treatment. In addition, cell cycle analysis revealed a growth arrest at phase G2/M within 24 hours post treatment, with cell killing represented by a sub-G1 population. Also, our  $\beta$ -galactosidase staining indicated that the surviving population showed signs of senescence following induced autophagy, as cells were enlarged and flattened. Taking into account that tumor cells need to evade the step of senescence to maintain growth [97], we found that the residual

surviving cells failed to recover after replenishment with drug-free medium for 15 days in an extended proliferative recovery study. All of these findings point toward an additional potential therapeutic outcome of stilbene 5c, preventing the re-growth of cancer cells after exposure.

#### *4.7 Antimetastatic and vascular disrupting properties of stilbene 5c*

Beside their roles in cell division and proliferation, microtubules play major functions in trafficking and migration in mammalian cells. Metastasized tumor cells require migration of cancer cells and formation of new blood vessels to enrich the tumor site with blood supply and oxygen for growth and development. Both of these processes are essentially mediated by microtubules and can be easily distorted by targeting tumor vasculature [98]. Several antiangiogenic studies have shown that these functions were abrogated by microtubule poisons [99-100]. In addition, two well-known colchicine-binding inhibitors have been identified as vascular-disrupting agents [101]. Another study indicated that stilbene 5c, a colchicine-site inhibitor, disrupts tumor vascular perfusion, but not the normal organ's blood supply [16]. In this regard, we have studied the antiangiogenic and antimetastatic properties of stilbene 5c and JG-03-14, microtubule poisons that bind to the colchicine-binding site, on B16/F10 melanoma in a syngeneic mouse model. While neither stilbene 5c nor JG-03-14 showed an antimetastatic effect according to the number of tumor nodules on the lungs, JG-03-14, but not the stilbene 5c, significantly reduced the volume of these nodules, indicating that JG-03-14 disrupts the vascular perfusion of tumor. Although the effect of stilbene 5c was barely remarkable but non-significant, we anticipate that higher doses of stilbene 5c are likely to disrupt tumor perfusion. The reason why JG-03-14 showed a significant effect could be due to either the higher dose used compared to stilbene 5c, or different pharmacokinetic properties. . This finding may indicate that both JG-03-14 and stilbene 5c are specific for angiogenesis via targeting endothelial cells as shown with combretastatin, an agent of the same group [16, 102].

#### 4.8 Future studies

Our results showed that the drug stilbene 5c induces multiple modes of cell death and growth in HCT116 colon carcinoma cells. These results led us to the next aims of this study in which inhibitors of autophagy and apoptosis can be used to investigate what modes of cell death are essentially induced. To further explain what primary cell killing mechanisms are responsible for the effects of stilbene 5c, we can utilize select pharmacological agents to inhibit the process of autophagy and determine how this would influence the toxicity of stilbene 5c. Chloroquine and Bafilomycin A-1 have been used to inhibit fusion of the autophagosome and lysosomes, preventing the last step of autophagy [103]. Also, we can transiently silence essential autophagy-regulating genes such as ATG5, ATG7, and Beclin-1. However, these approaches to inhibit autophagy might not clarify the exact role of autophagy due to the appearance of other mechanisms of cell death concurrently with autophagy i.e. shutting down one mechanism will enforce cells to die via another pathway.

In additional experiments, use of inhibitors of caspase cleavage, which would block the induction of apoptosis, could identify the contribution of apoptosis to drug action. Based on our results, we found that apoptosis was induced after the appearance of other modes of cell death. This may illustrate for us that promotion of apoptosis is a consequence of excessive stress. Thus, using Z-Vad may allow us to differentiate between cytotoxic and cytoprotective roles of autophagy in HCT116 cells.

It would be useful if we also assessed apoptotic cell death and mitotic catastrophe in p53-null HCT116 cells. We found that stilbene 5c induces both cell death and autophagy in p53-knock out HCT116 cells. We can perform DAPI and TUNEL assays to assess apoptotic cell death in p53-deficient cells. However, Annexin V staining could be useful to quantify numbers of cells undergoing apoptosis. Moreover, it would be worthwhile to perform Hoechst staining to evaluate the intensity of mitotic



catastrophe induction in p53 (-/-) HCT116 cells. These suggested assays and studies may clearly answer the question of what primary modes of cell death are particularly induced by stilbene 5c.

Finally, we would evaluate the effectiveness of stilbene 5c on HCT116 colon cancer cells *in vivo*, using an orthotopic model [104]. In the previous studies of stilbene 5c, the drug showed efficacy against HL60 and U937 cells *in vivo* [15]. IV injections of this drug at doses of 10, 50, and 100 mg/kg resulted in 22, 62 and 58% apoptosis respectively. In addition, 100 mg/kg of drug extensively killed central tumor cells with permitting the survival of viable cells at the peripheral areas of the tumor [16]. In this *in vivo* study, stilbene 5c was found to be tolerated in mice at doses as high as 100 mg/kg, indicating that stilbene 5c could be a promising VDA due to its low cardiotoxicity. Taken together, the anti-proliferative and the vascular disrupting properties may suggest that stilbene 5c is an effective agent for the therapy colon cancer.

1. Siegel, R., D. Naishadham, and A. Jemal, *Cancer statistics, 2012*. CA Cancer J Clin, 2012. **62**(1): p. 10-29.
2. Yokoi, K., et al., *Dual inhibition of epidermal growth factor receptor and vascular endothelial growth factor receptor phosphorylation by AEE788 reduces growth and metastasis of human colon carcinoma in an orthotopic nude mouse model*. Cancer Res, 2005. **65**(9): p. 3716-25.
3. Schmidt, M. and H. Bastians, *Mitotic drug targets and the development of novel anti-mitotic anticancer drugs*. Drug Resist Updat, 2007. **10**(4-5): p. 162-81.
4. Jiang, N., et al., *Advances in mitotic inhibitors for cancer treatment*. Mini Rev Med Chem, 2006. **6**(8): p. 885-95.
5. Dowlati, A., et al., *A phase I pharmacokinetic and translational study of the novel vascular targeting agent combretastatin a-4 phosphate on a single-dose intravenous schedule in patients with advanced cancer*. Cancer Res, 2002. **62**(12): p. 3408-16.
6. Stevenson, J.P., et al., *Phase I trial of the antivascular agent combretastatin A4 phosphate on a 5-day schedule to patients with cancer: magnetic resonance imaging evidence for altered tumor blood flow*. J Clin Oncol, 2003. **21**(23): p. 4428-38.
7. Rustin, G.J., et al., *Phase I clinical trial of weekly combretastatin A4 phosphate: clinical and pharmacokinetic results*. J Clin Oncol, 2003. **21**(15): p. 2815-22.
8. Beerepoot, L.V., et al., *Phase I clinical evaluation of weekly administration of the novel vascular-targeting agent, ZD6126, in patients with solid tumors*. J Clin Oncol, 2006. **24**(10): p. 1491-8.
9. Pace-Asciak, C.R., et al., *The red wine phenolics trans-resveratrol and quercetin block human platelet aggregation and eicosanoid synthesis: implications for protection against coronary heart disease*. Clin Chim Acta, 1995. **235**(2): p. 207-19.
10. Larrosa, M., F.A. Tomas-Barberan, and J.C. Espin, *The grape and wine polyphenol piceatannol is a potent inducer of apoptosis in human SK-Mel-28 melanoma cells*. Eur J Nutr, 2004. **43**(5): p. 275-84.
11. Holwell, S.E., et al., *Combretastatin A-1 phosphate a novel tubulin-binding agent with in vivo anti vascular effects in experimental tumours*. Anticancer Res, 2002. **22**(2A): p. 707-11.
12. Simoni, D., et al., *Design, synthesis and biological evaluation of novel stilbene-based antitumor agents*. Bioorg Med Chem, 2009. **17**(2): p. 512-22.
13. Roberti, M., et al., *Synthesis and biological evaluation of resveratrol and analogues as apoptosis-inducing agents*. J Med Chem, 2003. **46**(16): p. 3546-54.
14. Durrant, D., et al., *Mechanism of cell death induced by cis-3, 4', 5-trimethoxy-3'-aminostilbene in ovarian cancer*. Gynecol Oncol, 2008. **110**(1): p. 110-7.
15. Cao, T.M., et al., *Stilbene derivatives that are colchicine-site microtubule inhibitors have antileukemic activity and minimal systemic toxicity*. Am J Hematol, 2008. **83**(5): p. 390-7.
16. Durrant, D., et al., *cis-3, 4', 5-Trimethoxy-3'-aminostilbene disrupts tumor vascular perfusion without damaging normal organ perfusion*. Cancer Chemother Pharmacol, 2009. **63**(2): p. 191-200.
17. Kerr, J.F., A.H. Wyllie, and A.R. Currie, *Apoptosis: a basic biological phenomenon with wide-ranging implications in tissue kinetics*. Br J Cancer, 1972. **26**(4): p. 239-57.
18. Norbury, C.J. and I.D. Hickson, *Cellular responses to DNA damage*. Annu Rev Pharmacol Toxicol, 2001. **41**: p. 367-401.
19. Majno, G. and I. Joris, *Apoptosis, oncosis, and necrosis. An overview of cell death*. Am J Pathol, 1995. **146**(1): p. 3-15.
20. Nijhawan, D., N. Honarpour, and X. Wang, *Apoptosis in neural development and disease*. Annu Rev Neurosci, 2000. **23**: p. 73-87.
21. Opferman, J.T. and S.J. Korsmeyer, *Apoptosis in the development and maintenance of the immune system*. Nat Immunol, 2003. **4**(5): p. 410-5.

22. Elmore, S., *Apoptosis: a review of programmed cell death*. *Toxicol Pathol*, 2007. **35**(4): p. 495-516.
23. Mizushima, N., et al., *Autophagy fights disease through cellular self-digestion*. *Nature*, 2008. **451**(7182): p. 1069-75.
24. Cuervo, A.M., *Autophagy: in sickness and in health*. *Trends Cell Biol*, 2004. **14**(2): p. 70-7.
25. Ciechanover, A., *Proteolysis: from the lysosome to ubiquitin and the proteasome*. *Nat Rev Mol Cell Biol*, 2005. **6**(1): p. 79-87.
26. Takacs-Vellai, K., et al., *Inactivation of the autophagy gene bec-1 triggers apoptotic cell death in C. elegans*. *Curr Biol*, 2005. **15**(16): p. 1513-7.
27. Levine, B. and J. Yuan, *Autophagy in cell death: an innocent convict?* *J Clin Invest*, 2005. **115**(10): p. 2679-88.
28. Ravikumar, B., et al., *Rapamycin pre-treatment protects against apoptosis*. *Hum Mol Genet*, 2006. **15**(7): p. 1209-16.
29. Yang, Z. and D.J. Klionsky, *Eaten alive: a history of macroautophagy*. *Nat Cell Biol*, 2010. **12**(9): p. 814-22.
30. Chen, Y. and D.J. Klionsky, *The regulation of autophagy - unanswered questions*. *J Cell Sci*, 2011. **124**(Pt 2): p. 161-70.
31. Chang, Y.Y. and T.P. Neufeld, *Autophagy takes flight in Drosophila*. *FEBS Lett*, 2010. **584**(7): p. 1342-9.
32. Yang, Z. and D.J. Klionsky, *Mammalian autophagy: core molecular machinery and signaling regulation*. *Curr Opin Cell Biol*, 2010. **22**(2): p. 124-31.
33. McPhee, C.K. and E.H. Baehrecke, *Autophagy in Drosophila melanogaster*. *Biochim Biophys Acta*, 2009. **1793**(9): p. 1452-60.
34. Yang, Z. and D.J. Klionsky, *An overview of the molecular mechanism of autophagy*. *Curr Top Microbiol Immunol*, 2009. **335**: p. 1-32.
35. Petiot, A., et al., *Distinct classes of phosphatidylinositol 3'-kinases are involved in signaling pathways that control macroautophagy in HT-29 cells*. *J Biol Chem*, 2000. **275**(2): p. 992-8.
36. Blommaert, E.F., et al., *The phosphatidylinositol 3-kinase inhibitors wortmannin and LY294002 inhibit autophagy in isolated rat hepatocytes*. *Eur J Biochem*, 1997. **243**(1-2): p. 240-6.
37. Vigneron, A. and K.H. Vousden, *p53, ROS and senescence in the control of aging*. *Aging (Albany NY)*, 2010. **2**(8): p. 471-4.
38. Hayflick, L., *The Limited in Vitro Lifetime of Human Diploid Cell Strains*. *Exp Cell Res*, 1965. **37**: p. 614-36.
39. Shay, J.W. and I.B. Roninson, *Hallmarks of senescence in carcinogenesis and cancer therapy*. *Oncogene*, 2004. **23**(16): p. 2919-33.
40. Vergel, M., et al., *Cellular senescence as a target in cancer control*. *J Aging Res*, 2010. **2011**: p. 725365.
41. Hanahan, D. and R.A. Weinberg, *The hallmarks of cancer*. *Cell*, 2000. **100**(1): p. 57-70.
42. Wright, W.E. and J.W. Shay, *Time, telomeres and tumours: is cellular senescence more than an anticancer mechanism?* *Trends Cell Biol*, 1995. **5**(8): p. 293-7.
43. Kipling, D., et al., *Telomere-dependent senescence*. *Nat Biotechnol*, 1999. **17**(4): p. 313-4.
44. Olovnikov, A.M., *A theory of marginotomy. The incomplete copying of template margin in enzymic synthesis of polynucleotides and biological significance of the phenomenon*. *J Theor Biol*, 1973. **41**(1): p. 181-90.
45. Campisi, J. and F. d'Adda di Fagagna, *Cellular senescence: when bad things happen to good cells*. *Nat Rev Mol Cell Biol*, 2007. **8**(9): p. 729-40.
46. Kamijo, T., et al., *Tumor suppression at the mouse INK4a locus mediated by the alternative reading frame product p19ARF*. *Cell*, 1997. **91**(5): p. 649-59.

47. Malumbres, M. and A. Carnero, *Cell cycle deregulation: a common motif in cancer*. Prog Cell Cycle Res, 2003. **5**: p. 5-18.
48. Ho, J.S., et al., *p53-Dependent transcriptional repression of c-myc is required for G1 cell cycle arrest*. Mol Cell Biol, 2005. **25**(17): p. 7423-31.
49. Di, X., et al., *Apoptosis, autophagy, accelerated senescence and reactive oxygen in the response of human breast tumor cells to adriamycin*. Biochem Pharmacol, 2009. **77**(7): p. 1139-50.
50. Gewirtz, D.A., S.E. Holt, and L.W. Elmore, *Accelerated senescence: an emerging role in tumor cell response to chemotherapy and radiation*. Biochem Pharmacol, 2008. **76**(8): p. 947-57.
51. Amati, B., K. Alevizopoulos, and J. Vlach, *Myc and the cell cycle*. Front Biosci, 1998. **3**: p. d250-68.
52. Harley, C.B., A.B. Futcher, and C.W. Greider, *Telomeres shorten during ageing of human fibroblasts*. Nature, 1990. **345**(6274): p. 458-60.
53. Bodnar, A.G., et al., *Extension of life-span by introduction of telomerase into normal human cells*. Science, 1998. **279**(5349): p. 349-52.
54. Takai, H., A. Smogorzewska, and T. de Lange, *DNA damage foci at dysfunctional telomeres*. Curr Biol, 2003. **13**(17): p. 1549-56.
55. Rodier, F., et al., *Persistent DNA damage signalling triggers senescence-associated inflammatory cytokine secretion*. Nat Cell Biol, 2009. **11**(8): p. 973-9.
56. Herbig, U., et al., *Telomere shortening triggers senescence of human cells through a pathway involving ATM, p53, and p21(CIP1), but not p16(INK4a)*. Mol Cell, 2004. **14**(4): p. 501-13.
57. Nakamura, A.J., et al., *Both telomeric and non-telomeric DNA damage are determinants of mammalian cellular senescence*. Epigenetics Chromatin, 2008. **1**(1): p. 6.
58. McConnell, B.B., et al., *Inhibitors of cyclin-dependent kinases induce features of replicative senescence in early passage human diploid fibroblasts*. Curr Biol, 1998. **8**(6): p. 351-4.
59. Ramirez, R.D., et al., *Putative telomere-independent mechanisms of replicative aging reflect inadequate growth conditions*. Genes Dev, 2001. **15**(4): p. 398-403.
60. Alimonti, A., et al., *A novel type of cellular senescence that can be enhanced in mouse models and human tumor xenografts to suppress prostate tumorigenesis*. J Clin Invest, 2010. **120**(3): p. 681-93.
61. Zachos, G., et al., *Chk1 is required for spindle checkpoint function*. Dev Cell, 2007. **12**(2): p. 247-60.
62. Petsalaki, E., et al., *Phosphorylation at serine 331 is required for Aurora B activation*. J Cell Biol, 2011. **195**(3): p. 449-66.
63. Portugal, J., S. Mansilla, and M. Bataller, *Mechanisms of drug-induced mitotic catastrophe in cancer cells*. Curr Pharm Des, 2010. **16**(1): p. 69-78.
64. Castedo, M., et al., *Cell death by mitotic catastrophe: a molecular definition*. Oncogene, 2004. **23**(16): p. 2825-37.
65. Castedo, M., et al., *Mitotic catastrophe constitutes a special case of apoptosis whose suppression entails aneuploidy*. Oncogene, 2004. **23**(25): p. 4362-70.
66. Bataller, M. and J. Portugal, *Apoptosis and cell recovery in response to oxidative stress in p53-deficient prostate carcinoma cells*. Arch Biochem Biophys, 2005. **437**(2): p. 151-8.
67. Mansilla, S., M. Bataller, and J. Portugal, *Mitotic catastrophe as a consequence of chemotherapy*. Anticancer Agents Med Chem, 2006. **6**(6): p. 589-602.
68. Eom, Y.W., et al., *Two distinct modes of cell death induced by doxorubicin: apoptosis and cell death through mitotic catastrophe accompanied by senescence-like phenotype*. Oncogene, 2005. **24**(30): p. 4765-77.
69. Niida, H., et al., *Depletion of Chk1 leads to premature activation of Cdc2-cyclin B and mitotic catastrophe*. J Biol Chem, 2005. **280**(47): p. 39246-52.

70. Brown, J.M. and L.D. Attardi, *The role of apoptosis in cancer development and treatment response*. Nat Rev Cancer, 2005. **5**(3): p. 231-7.
71. Roninson, I.B., E.V. Broude, and B.D. Chang, *If not apoptosis, then what? Treatment-induced senescence and mitotic catastrophe in tumor cells*. Drug Resist Updat, 2001. **4**(5): p. 303-13.
72. Hernandez-Vargas, H., J. Palacios, and G. Moreno-Bueno, *Telling cells how to die: docetaxel therapy in cancer cell lines*. Cell Cycle, 2007. **6**(7): p. 780-3.
73. Bampton, E.T., et al., *The dynamics of autophagy visualized in live cells: from autophagosome formation to fusion with endo/lysosomes*. Autophagy, 2005. **1**(1): p. 23-36.
74. Young, A.R., et al., *Autophagy mediates the mitotic senescence transition*. Genes Dev, 2009. **23**(7): p. 798-803.
75. Guo, J.Y., et al., *Activated Ras requires autophagy to maintain oxidative metabolism and tumorigenesis*. Genes Dev, 2011. **25**(5): p. 460-70.
76. Komatsu, M., et al., *Homeostatic levels of p62 control cytoplasmic inclusion body formation in autophagy-deficient mice*. Cell, 2007. **131**(6): p. 1149-63.
77. Vogel, C., C. Hager, and H. Bastians, *Mechanisms of mitotic cell death induced by chemotherapy-mediated G2 checkpoint abrogation*. Cancer Res, 2007. **67**(1): p. 339-45.
78. Chatterji, B.P., et al., *Microtubules as antifungal and antiparasitic drug targets*. Expert Opin Ther Pat, 2011. **21**(2): p. 167-86.
79. Pajk, B., et al., *Anti-tumor activity of capecitabine and vinorelbine in patients with anthracycline- and taxane-pretreated metastatic breast cancer: findings from the EORTC 10001 randomized phase II trial*. Breast, 2008. **17**(2): p. 180-5.
80. Norris, B., et al., *Phase III comparative study of vinorelbine combined with doxorubicin versus doxorubicin alone in disseminated metastatic/recurrent breast cancer: National Cancer Institute of Canada Clinical Trials Group Study MA8*. J Clin Oncol, 2000. **18**(12): p. 2385-94.
81. Dimitroulis, J. and G.P. Stathopoulos, *Evolution of non-small cell lung cancer chemotherapy (Review)*. Oncol Rep, 2005. **13**(5): p. 923-30.
82. Prabhudesai, S.G., et al., *Apoptosis and chemo-resistance in colorectal cancer*. J Surg Oncol, 2007. **96**(1): p. 77-88.
83. Tao, W., *The mitotic checkpoint in cancer therapy*. Cell Cycle, 2005. **4**(11): p. 1495-9.
84. Jordan, M.A., et al., *Mitotic block induced in HeLa cells by low concentrations of paclitaxel (Taxol) results in abnormal mitotic exit and apoptotic cell death*. Cancer Res, 1996. **56**(4): p. 816-25.
85. Milross, C.G., et al., *Relationship of mitotic arrest and apoptosis to antitumor effect of paclitaxel*. J Natl Cancer Inst, 1996. **88**(18): p. 1308-14.
86. Nabha, S.M., et al., *Combretastatin-A4 prodrug induces mitotic catastrophe in chronic lymphocytic leukemia cell line independent of caspase activation and poly(ADP-ribose) polymerase cleavage*. Clin Cancer Res, 2002. **8**(8): p. 2735-41.
87. Castedo, M., et al., *The cell cycle checkpoint kinase Chk2 is a negative regulator of mitotic catastrophe*. Oncogene, 2004. **23**(25): p. 4353-61.
88. Tao, W., et al., *Induction of apoptosis by an inhibitor of the mitotic kinesin KSP requires both activation of the spindle assembly checkpoint and mitotic slippage*. Cancer Cell, 2005. **8**(1): p. 49-59.
89. Rothbart, S.B., A.C. Racanelli, and R.G. Moran, *Pemetrexed indirectly activates the metabolic kinase AMPK in human carcinomas*. Cancer Res, 2010. **70**(24): p. 10299-309.
90. Kochl, R., et al., *Microtubules facilitate autophagosome formation and fusion of autophagosomes with endosomes*. Traffic, 2006. **7**(2): p. 129-45.
91. Asanuma, K., et al., *MAP-LC3, a promising autophagosomal marker, is processed during the differentiation and recovery of podocytes from PAN nephrosis*. FASEB J, 2003. **17**(9): p. 1165-7.

92. Mosieniak, G., et al., *Curcumin induces permanent growth arrest of human colon cancer cells: Link between senescence and autophagy*. Mech Ageing Dev, 2012.
93. Ding, W.X., et al., *Differential effects of endoplasmic reticulum stress-induced autophagy on cell survival*. J Biol Chem, 2007. **282**(7): p. 4702-10.
94. Yousefi, S., et al., *Calpain-mediated cleavage of Atg5 switches autophagy to apoptosis*. Nat Cell Biol, 2006. **8**(10): p. 1124-32.
95. Pyo, J.O., et al., *Essential roles of Atg5 and FADD in autophagic cell death: dissection of autophagic cell death into vacuole formation and cell death*. J Biol Chem, 2005. **280**(21): p. 20722-9.
96. Lu, Z., et al., *The tumor suppressor gene ARHI regulates autophagy and tumor dormancy in human ovarian cancer cells*. J Clin Invest, 2008. **118**(12): p. 3917-29.
97. Zhang, H., *Molecular signaling and genetic pathways of senescence: Its role in tumorigenesis and aging*. J Cell Physiol, 2007. **210**(3): p. 567-74.
98. Tozer, G.M., C. Kanthou, and B.C. Baguley, *Disrupting tumour blood vessels*. Nat Rev Cancer, 2005. **5**(6): p. 423-35.
99. Jordan, M.A. and K. Kamath, *How do microtubule-targeted drugs work? An overview*. Curr Cancer Drug Targets, 2007. **7**(8): p. 730-42.
100. Lippert, J.W., 3rd, *Vascular disrupting agents*. Bioorg Med Chem, 2007. **15**(2): p. 605-15.
101. Griggs, J., J.C. Metcalfe, and R. Hesketh, *Targeting tumour vasculature: the development of combretastatin A4*. Lancet Oncol, 2001. **2**(2): p. 82-7.
102. Kanthou, C. and G.M. Tozer, *The tumor vascular targeting agent combretastatin A-4-phosphate induces reorganization of the actin cytoskeleton and early membrane blebbing in human endothelial cells*. Blood, 2002. **99**(6): p. 2060-9.
103. Shintani, T. and D.J. Klionsky, *Autophagy in health and disease: a double-edged sword*. Science, 2004. **306**(5698): p. 990-5.
104. Rajput, A., et al., *Characterization of HCT116 human colon cancer cells in an orthotopic model*. J Surg Res, 2008. **147**(2): p. 276-81.